Novel Hyperspectral Sun Photometer for Satellite Remote Sensing Data Radiometric Calibration and Atmospheric Aerosol Studies

Mary Pagnutti, Robert E. Ryan, Kara Holekamp, Gary Harrington
Science Systems and Applications, Inc.
John C. Stennis Space Center, Mississippi

Troy Frisbie
Applied Sciences Directorate
National Aeronautics and Space Administration
John C. Stennis Space Center, Mississippi

National Aeronautics and
Space Administration

John C. Stennis Space Center
SSC, Mississippi 39529–6000

January 2006

Novel Hyperspectral Sun Photometer for Satellite Remote Sensing Data Radiometric Calibration and Atmospheric Aerosol Studies

Acknowledgments

This report is a joint work of employees of the National Aeronautics and Space Administration and employees of Science Systems and Applications, Inc., under Task Order NNS04AB54T with the National Aeronautics and Space Administration.

Trade names and trademarks are used in this report for identification only. Their usage does not constitute an official endorsement, either expressed or implied, by the National Aeronautics and Space Administration.

Table of Contents

Tables

Figures

Executive Summary

In this project, a simple and cost-effective, hyperspectral sun photometer for radiometric vicarious remote sensing system calibration, air quality monitoring, and potentially in-situ planetary climatological studies, was developed. The device was constructed solely from off the shelf components and was designed to be easily deployable for support of short-term verification and validation data collects. This sun photometer not only provides the same data products as existing multi-band sun photometers but also the potential of hyperspectral optical depth and diffuse-to-global products. As compared to traditional sun photometers, this device requires a simpler setup, less data acquisition time and allows for a more direct calibration approach. Fielding this instrument has also enabled Stennis Space Center (SSC) Applied Sciences Directorate personnel to cross-calibrate existing sun photometers. This innovative research will position SSC personnel to perform air quality assessments in support of the NASA Applied Sciences Program's National Applications program element as well as to develop techniques to evaluate aerosols in a Martian or other planetary atmosphere.

This page intentionally blank

1.0 Background

Various sun photometers measure several components of solar irradiance including total (or global), direct and diffuse, at the altitude from which they are operated. By carefully selecting the wavelengths at which measurements will be taken, sun photometer data can be analyzed to estimate the molecular scattering, aerosol extinction, columnar water vapor, ozone, and other trace gases in the atmosphere at the observation time (Reagan et al., 1986). This type of information is used in atmospheric and pollution studies as well as radiometric calibration of remote sensing systems. Sun photometers are used worldwide to assess the influence of aerosols on satellite remotely sensed data and climate forcing (Holben et al., 1992). These devices are also being considered for planetary climatological studies.

Ground based sun photometers are also critical for developing correlations between remotely sensed optical depth measurements and other ground based aerosol measurements. When used for this purpose, sun photometers can be fielded for extended periods and are exposed continuously to ultraviolet radiation and contaminants such as dust and precipitation condensates, which will degrade performance over time (Reagan et al., 1986).

The NASA Applied Sciences Directorate (ASD) at Stennis Space Center (SSC) owns and operates several traditional sun photometers including University of Arizona Automated Solar Radiometers (ASRs) (Reagan et al., 1992), shown in Figure 1, and Yankee Environmental Systems, Inc., Multifilter Rotating Shadowband Radiometers (MFRSRs) (Harrison et al., 1994), shown in Figure 2, as part of its verification and validation (V&V) program (Pagnutti et al., 2002; Pagnutti et al., 2003). These devices primarily support atmospheric monitoring for the radiometric characterization of satellite-based high spatial resolution commercial imaging products and have supported the development of calibration coefficients that GeoEye (formally Space Imaging and ORBIMAGE) and DigitalGlobe have used to update their radiometric calibration coefficients (Zanoni, 2003). Accurate data from the sun photometers are essential to the success of these calibration exercises. Significant resources are required to calibrate, maintain, acquire, and process data from these traditional sun photometers.

Figure 1. Automated Solar Radiometer.

Figure 2. MultiFilter Rotating Shadowband Radiometer.

The ASR measures the direct solar irradiance in 10 narrow band channels in the visible through near-infrared spectral region for which the center wavelengths are shown in Table 1. After an initial solar alignment, the device automatically tracks the sun throughout the data acquisition period. This instrument typically takes data every minute and nods itself away from the sun to reduce ultraviolet exposure.

Table 1. Traditional sun photometer operating bands.

ASR Bands	MFRSR Bands
380 nm	
400 nm	415 nm
440 nm	
520 nm	500 nm
610 nm	615 nm
670 nm	673 nm
780 nm	
870 nm	870 nm
940 nm	940 nm
1030 nm	

The MFRSR measures the total and diffuse components of solar irradiance in one broadband and six different narrow band channels, for which the center wavelengths are shown in Table 1, in the visible through near-infrared spectral region. The direct component is estimated from subtracting the diffuse component from the total irradiance. A microprocessor-controlled shadowband (curved metal strip) alternately shades and exposes the instrument diffuser, which allows the device to measure both irradiance components with only one instrument.

1.1 Sun Photometer Data Measurements

The total solar irradiance E_{total} at a surface consists of a direct component E_{direct} (associated with the transmission of extraterrestrial solar irradiance E_0 to the surface) and a diffuse component $E_{diffuse}$ from the atmosphere. Total solar irradiance can therefore be written as:

$$E_{total} = E_{direct} + E_{diffuse} \tag{1}$$

Using the fact that Beer's Law holds in many cases (except for some molecular bands) for E_{direct}, the total solar irradiance can be written for any wavelength as:

$$E_{total} = E_0 e^{-\tau m} + E_{diffuse} \tag{2}$$

where τ is the vertical optical thickness of the atmosphere, and m is the relative air mass described as the ratio of the atmospheric optical thickness along a line of sight to the sun to the vertical atmospheric optical thickness.

The most common sun photometer data product is direct solar irradiance E_{direct}. E_{direct} is measured directly by the ASR sun photometer and is estimated by subtracting the diffuse component of the total irradiance from the total irradiance measurement with the MFRSR sun photometer.

Focusing on direct irradiance, only the first term of Equation (2) is examined. This term can be transformed to a linear expression by taking the natural log as shown in Equation (3).

$$\ln(E_{direct}) = \ln(E_0) - \tau m \tag{3}$$

Sun photometer detector and amplifier output voltage V is linearly related with irradiance E. The output voltage is digitized to a digital number (DN) to enable computer processing of the data. Therefore, DN

is linearly related to irradiance E. The extraterrestrial solar irradiance E_0 is dependent on the square of the relative sun-earth distance R_S measured in astronomical units. Thus, using the relationships given above, E_0 can be related to DN_0, which is the sun photometer calibration constant, or the digital number at R_S=1 at the top-of-atmosphere (m=0). Rewriting Equation (3) in terms of DN gives Equation (4).

$$\ln(DN) = \ln\left(\frac{DN_0}{R_S^2}\right) - \tau m \tag{4}$$

1.2 Traditional Sun Photometer Calibration

Traditional sun photometers are calibrated using the Langley regression method (Harrison and Michalsky, 1994). Using this method, the calibration constant DN_0 introduced above, is estimated by observing the sun photometer output voltage, converted to DN, over a large change of air mass. This typically takes several hours from either daybreak to solar noon or solar noon to dusk. Data pairs of (m, $\ln(DN)$) are generated, plotted, and extrapolated to an air mass value of zero. Optical depth is then estimated from the slope, τ, of the dataset. τ and DN are written as:

$$DN_0 = R_S^2\, DN_{m=0} \qquad \text{and} \qquad \tau = \frac{\ln(DN_{m=0}) - \ln(DN)}{m} \tag{5}$$

DN_0 and τ can therefore be solved knowing R_S and m. Air mass m can be estimated in several ways. A common method is to use expressions that require the zenith angle to the sun (Kasten et al., 1989). The zenith angles can be estimated from astronomical expressions using date, time, latitude, and longitude information. Air mass can also be estimated by using a radiative transfer code, such as Moderate Resolution Transmittance (MODTRAN) (Berk et al., 1999). R_S can be found using general astronomical information (Stern, 2005; Cornell University, 2005) and knowledge of perihelion dates (U.S. Naval Observatory, 2005). DN is related to E_0 through knowledge of the exoatmospheric irradiance.

Sun photometer calibration is typically performed by placing the sun photometer at a high altitude location, such as a mountaintop, for several days, preferably at a time of year when there are few clouds (O'Neill et al., 1984). Langley regression analyses are performed on the data to generate the calibration coefficients. This process generally requires that the sun photometer be taken out of service for several months and shipped to a distant location. The calibration is typically better than 2 percent for the visible through near-infrared spectral range. The University of Arizona recommends ASR mountaintop calibrations to be performed at least annually. Calibration errors, however, can grow much larger than 2 percent for other sun photometers such as MFRSRs. These sun photometers require routine Langley regression analyses to maintain calibration. Every time the ASRs and MFRSRs are fielded for sensor characterizations, SSC ASD personnel perform a Langley regression to identify and track instrument drift.

Ground-based sun photometers are critical for developing correlations between remotely sensed optical depth measurements and other ground-based aerosol measurements. When used for this purpose, sun

photometers are fielded for extended periods and are exposed continuously to ultraviolet radiation, which will also degrade performance over time.

This Langley calibration approach may also be impractical and inadequate for maintaining sun photometer calibration for places in the world where the atmosphere is harsh and/or variable. In the case of a Martian atmosphere, dust will further degrade sun photometer performance. Another measurement approach that does not require hours of data acquisition will be needed to protect the optics and maintain calibration.

2.0 Novel Sun Photometer

In this project, an innovative, yet cost-effective, hyperspectral sun photometer was developed. The device was constructed solely from off the shelf components and was designed to be easily deployable for support of short term V&V data collects. This novel sun photometer not only provides the same data products as existing sun photometers, it also provides new types of data not previously available. As compared to traditional field instruments, this sun photometer requires a simpler setup and less data acquisition time. It also allows for a more direct calibration approach, unlike the Langley regression analysis currently performed on traditional sun photometer data as described above.

2.1 Approach

The novel sun photometer estimates the direct solar irradiance E_{direct} by taking two measurements of a highly reflective near-Lambertian surface with a laboratory calibrated spectroradiometer. Total radiance, L_{total}, of a solar illuminated highly reflective Lambertian surface is first measured by the spectroradiometer. The diffuse component of total radiance, $L_{diffuse}$, is then measured by shadowing and re-measuring the same surface. The shadowing blocks only a few degrees of the sky, allowing nearly the entire diffuse component of the total radiance to strike the surface and then to be measured. In this way the measurements are similar to the MFRSR described above. Direct solar radiance is first found from the difference of these two measurements:

$$L_{direct} = L_{total} - L_{diffuse} \tag{6}$$

Knowing the reflectance factor of the near-Lambertian surface, $\rho(\theta,\varphi)$, as a function of solar zenith angle θ and solar azimuth angle φ, direct solar irradiance can be determined by:

$$E_{direct} = \frac{\pi L_{direct}}{\rho(\theta,\varphi)\cos(\theta)} \tag{7}$$

With careful measurements, the irradiance can determined to accuracies better than 2-3 percent, which is comparable to the traditional method discussed above.

Rewriting Equation (3), optical depth can be determined as:

$$\tau = \frac{\ln(E_0) - \ln(E_{direct})}{m} \tag{8}$$

The air mass, m, in this expression can be estimated as described above in Section 1.2. The extraterrestrial solar irradiance, E_0, is available from careful measurements that have been incorporated into radiative transfer codes, such as MODTRAN.

2.2 Implementation

The novel sun photometer developed under this Center Director Discretionary Fund project is shown in Figure 3. The two primary components of the concept are an Analytical Spectral Devices, Inc., full range (FR) spectroradiometer and a highly reflective near-Lambertian National Institute of Standards and Technology (NIST) traceable calibrated Spectralon® plaque, both of which come from the SSC V&V instrumentation suite. The spectroradiometer fiber, probe, and eight-degree optic are attached to a fixture pointed down at right angles to and centered directly over the Spectralon plaque. The Spectralon plaque is stationary and mounted on a tripod. The spectroradiometer backpack, electronics, and computer rest alongside the tripod.

Figure 3. Novel sun photometer.

Table 2 gives an overview of the tasks associated with developing and evaluating data taken from the novel sun photometer proof-of-concept device. These tasks are described in more detail in the following sections.

Table 2. Novel sun photometer project tasks.

Task	Description
1	Perform radiometric calibration of spectroradiometer. Characterize Spectralon plaques for reflectance factor.
2	Develop simple method for shadowing Spectralon plaques.
3	Develop processing software (based on previous work) to extract optical depth for simple comparison with existing sun photometer data in MATLAB®.
4	Take coincident data with calibrated sun photometers on clear days associated with satellite remote sensing system calibrations.
5	Process new sun photometer datasets and compare with conventional sun photometer results.
6	Document results in a final report.

2.2.1 Spectroradiometer Calibration

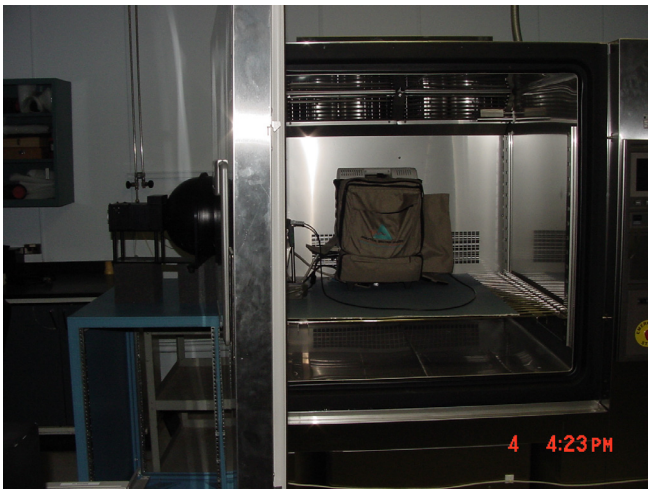

Figure 4. Spectroradiometer radiometric calibration inside environmental chamber.

The novel sun photometer proof-of-concept incorporates a SSC-owned Analytical Spectral Devices, Inc., FR spectroradiometer operating from 350–2500 nm with approximately 10 nm or better spectral resolution over the entire spectral range. The spectroradiometer was calibrated with a SSC NIST traceable integrating sphere accurate to better than 2 percent over most of the spectral range. The spectroradiometer calibration was performed in an environmental chamber to ascertain drifts associated with temperature. Calibration data was acquired at four different temperatures (4, 14, 24, and 34 ºC) that span the expected ambient temperature range that the spectroradiometer would be operating in. Figure 4 shows the spectroradiometer acquiring data within the environmental chamber.

2.2.2 Spectralon Characterization

The novel sun photometer also incorporates a 99 percent reflective Spectralon plaque. Reflectance measurements were made of the Spectralon plaque in the SSC Instrument Validation Laboratory prior to incorporation into the sun photometer, as shown in Figure 5. All measurements were taken at a light source (solar) incidence angle of 45°. These measurements were then compared to measurements taken on an identical SSC Spectralon plaque at NIST. The Jackson Spectralon reflectance model (Jackson et al., 1992) was used to calculate bidirectional reflectance distribution function (BRDF) values at solar incident angles corresponding to conditions present during sun photometer field acquisitions.

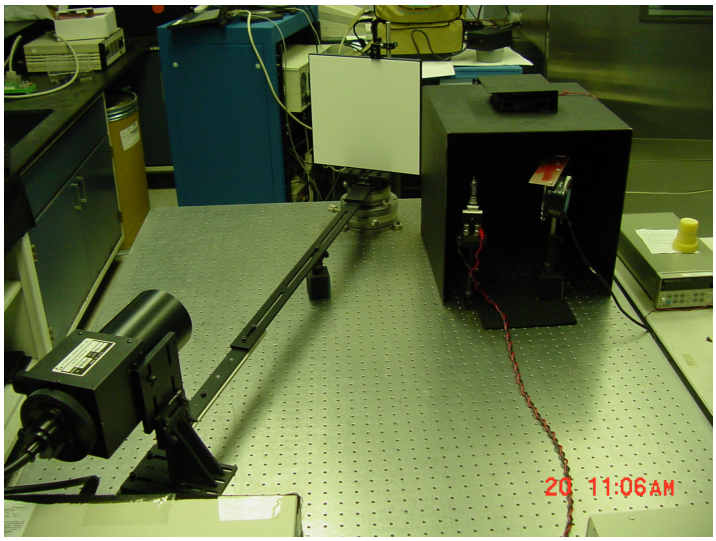

Figure 5. Spectralon plaque BRDF measurement.

2.2.3 Spectralon Shadowing Method/Algorithm

As described in above in Section 2.0, the novel sun photometer concept requires two types of measurements to be taken with the spectroradiometer. The first, L_{total}, is accomplished by acquiring spectroradiometer measurements of the 99 percent reflective Spectralon plaque while it is fully illuminated by the sun. The second measurement, $L_{diffuse}$, is accomplished by taking a series of three Spectralon measurements with the spectroradiometer. In the first of these measurements, a shade is positioned over the Spectralon plaque. This measurement by itself does not represent $L_{diffuse}$, but rather $L^*_{diffuse}$ because the shade not only shades the Spectralon plaque, but also blocks out a portion of the sky. To account for this unwanted effect, two additional measurements are made while blocking the same amount of sky without shading the plaque, in a manner similar to the operation of the MFRSR. The first measurement, L_{left}, is taken while the shade blocks the sky and casts a shadow to the left of the panel, and the second, L_{right}, is taken while the shade blocks the sky and casts a shadow to the right of the panel. Blocked sky radiance can then be quantified by averaging the two measurements and subtracting them from L_{total}. This value is added back into $L^*_{diffuse}$ to obtain $L_{diffuse}$ as shown below in Equation (9) (Harrison et al., 1994).

$$L_{diffuse} = L^*_{diffuse} + \left(L_{total} - \frac{L_{left} + L_{right}}{2} \right) \tag{9}$$

2.2.4 Processing Software

Software was developed in MATLAB to extract several atmospheric parameters that could then be compared to those obtained with traditional sun photometers. Total radiance, L_{total}, was measured directly by the novel sun photometer as described above. Software was written based on Equations (6) and (9) to determine $L_{diffuse}$ and L_{direct}. The values $L_{diffuse}$ and L_{total} were ratioed to obtain the diffuse-to-global ratio (D2G). Knowing the Spectralon plaque reflectance, including BRDF effects, the solar azimuth, φ, and zenith, θ, angles, the extraterrestrial irradiance, E_0, from MODTRAN, and Equations (7) and (8), software was written to obtain the atmospheric optical thickness τ. These two parameters, D2G and τ, were then used to validate the performance of the novel sun photometer.

3.0 Results

The novel sun photometer developed under this Center Director's Discretionary Fund (CDDF) project was fielded alongside conventional sun photometers. At least one ASR and one MFRSR were fielded each time the novel sun photometer acquired data. Atmospheric optical depths, τ, were calculated based on measured parameters from each sun photometer and compared. In addition, estimates of molecular scattering, measured as diffuse-to-global ratios ($L_{diffuse} / L_{total}$), were calculated based on the novel sun photometer measurements and compared to those calculated using MFRSRs. These calculations were all done on a per-band basis (based on most of the conventional sun photometer bands described in Table 1) multiple times throughout each field campaign.

3.1 Acquired Datasets

A test case matrix was developed to test the ability of the novel sun photometer to generate values typically measured by traditional sun photometers. Five ground data acquisition dates for which sufficient novel sun photometer measurements existed were selected. These dates leveraged field campaigns that had conventional sun photometers already fielded.

Table 3 identifies the conventional sun photometers fielded by serial number for each ground data acquisition date. It also identifies the number of times data was acquired by the novel sun photometer. (During each field campaign, data was acquired continuously by both the ASRs and MFRSRs). In total, 67 test cases were evaluated. Each test case compared optical depth, as determined by the novel sun photometer, with that determined by either an MFRSR or an ASR. Test cases involving MFRSR comparisons also include a comparison of D2G.

Table 3. Test case evaluations.

Date	Location	Traditional Sun Photometer	No. of Novel Sun Photometer Datasets Acquired	No. of Test Cases (Type of Comparison)
9/17/03	SSC	ASR 27 MFRSR 451 MFRSR 477	5	5 (τ) 5 (τ + D2G) 5 (τ + D2G)
9/28/03	SSC	ASR 27 MFRSR 451 MFRSR 477	2	2 (τ) 2 (τ + D2G) 2 (τ + D2G)
1/10/04	SSC	ASR 27 MFRSR 477	2	2 (τ) 2 (τ + D2G)
12/15/04	SSC	ASR 25 ASR 27 MFRSR 451 MFRSR 477	6	6 (τ) 6 (τ) 6 (τ + D2G) 6 (τ + D2G)
4/27/05	SSC	ASR 25 ASR 27 MFRSR 477	6	6 (τ) 6 (τ) 6 (τ + D2G)

3.2 Results as Compared to Traditional Sun Photometers

Optical depth values were generated from both types of traditional sun photometers and from the novel sun photometer for each instrument spectral band for each test case. D2G ratios were also generated from the MFRSRs and the novel sun photometer for each instrument spectral band test for each test case. To give one measure of accuracy per test case, a root mean square (RMS) error was found for each case over the instrument bands (ASR bands 1 to 8, MFRSR bands 1 to 5), described in Table 1. The 940 and 1030 nm bands were not utilized in this evaluation. The 940 nm band is a water vapor band, and the 1030 nm band is near a transition area in the ASD spectroradiometer. These RMS values were then averaged across the multiple times the novel sun photometer acquired data, to give an average RMS for each date/sun

photometer/type of measurement combination. These average RMS values are given below in Table 4. The table shows that with the exception of data acquired on September 28, 2003, the average root mean square errors were less than .07 and typically less than .03. Anomalies associated with the dataset of September 28 are described below. Individual atmospheric optical depth and diffuse to global comparisons for each instrument, date, time, and band are detailed in Appendix A.

To assess the impact of these atmospheric optical thickness differences on remote sensing V&V activities, top of atmosphere (TOA) radiances were determined for several targets within a scene. The TOA radiances were based on the newly calculated atmospheric optical thickness and then compared to radiance values based on atmospheric optical thickness values obtained with traditional sun photometers. Data were evaluated from three days representing varied visibilities: September 28, 2003; January 10, 2004; and April 27, 2005. The optical depths generated using both the novel sun photometer and the conventional ASR were used to generate two MODTRAN radiative transport code input parameters (VISIBILITY and IHAZE). MODTRAN was then used to estimate the TOA radiance values over several targets measured as part of each day's ground truthing campaign. Table 4 details the differences in the MODTRAN input parameters (VISIBILITY and IHAZE) along with the TOA radiance values obtained using both the traditional ASR and the novel sun photometer data. Radiance values in the table are in units of $W/(m^2 sr\mu)$. The targets identified in the table are the 52 percent, 22 percent, and 3.5 percent reflectance calibration tarps, a rye grass field in an area known as Big Level Mississippi (BL), and two sandy areas associated with gravel mining in southern Mississippi (DG and Perk).

As before when looking at the differences in atmospheric optical depth, large differences are seen when comparing TOA radiances calculated using the novel sun photometer as compared to traditional sun photometers for September 28, 2003. Differences between TOA radiance as estimated using traditional sun photometers and the novel sun photometer in the other two days are negligible.

The TOA radiance data that was based on traditional sun photometer and ground reflectance data obtained on September 28, 2003, was used to characterize OrbView-3 imagery. The original plots summarizing OrbView-3 radiometric accuracy are shown in Figure 6. This figure shows significant scatter between TOA radiance results obtained on October 20, 2003, and September 28, 2003. When the TOA radiance results for September 28 are replaced with updated results obtained using the novel sun photometer, the scatter is significantly reduced, as shown in Figure 7. Looking closely at the atmospheric conditions present on September 28, it became apparent that there were several instances when cloud cover influenced the sun photometer data obtained during the morning hours prior to the satellite overpass. The Langley regression analysis, which takes into account data acquired from sunrise to solar noon, was likely affected by the early morning intermittent cloud cover. The novel sun photometer, which depends on field data obtained solely during the satellite overpass, was not affected.

3.3 Novel Sun Photometer Calibration

A method was developed to calibrate the novel sun photometer in the field in a way that does not depend on Langley regression analysis as with traditional sun photometers. The calibration technique involves radiometrically calibrating the spectroradiometer, which measures absolute radiance above a Spectralon plaque. The calibration technique follows the same general method that is used in traditional laboratory

calibrations. Many V&V teams field spectroradiometers to measure target reflectance during measurement campaigns, but they do not require this type of field calibration. This is because the spectroradiometers that are currently fielded measure reflectance rather than absolute radiance, as they do with the novel sun photometer.

Traditional laboratory radiometric calibrations of spectroradiometers are performed by measuring the absolute radiance and reflectance off a uniform Lambertian source, generated by illuminating an integrating sphere with a tungsten halogen lamp. These sources cost tens of thousands of dollars, are power intensive, large, and not practical to place in the field. Unfortunately, calibrations made in the laboratory prior to a measurement campaign do not necessarily hold in the field due to instrument drift. To meet this need, a low power, portable calibration system, which incorporates light emitting diodes (LEDs) illuminating an integrating sphere, was developed. The high efficiency of LEDs and compact power supplies enables this new type of field calibration source. Although an LED output can drift with temperature and current, the new calibration device sufficiently controls the LED temperature and current.

Table 4. Differences in TOA radiance values obtained using conventional sun photometers and the novel sun photometer.

Date	Original VISIBILITY / IHAZE[1]	New VISIBILITY / IHAZE[2]	Targets	Bands	Original Radiance	New Radiance	Percent Difference
9/28/03	21 / 5	138 / 4	52%	Blue	167.56	234.56	-39.99 %
				Green	157.43	216.71	-37.65 %
				Red	142.05	188.34	-32.59 %
				NIR	108.05	132.46	-22.59 %
			22%	Blue	102.16	130.27	-27.52 %
				Green	86.879	111.29	-28.10 %
				Red	72.438	90.950	-25.56 %
				NIR	51.999	60.091	-15.56 %
			3.5%	Blue	52.286	50.728	2.98 %
				Green	34.292	32.704	4.63 %
				Red	22.533	21.127	6.24 %
				NIR	15.332	12.731	16.96 %
1/10/04	119 / 1	184 / 1	52%	Blue	151.83	153.10	-0.84 %
				Green	143.80	145.33	-1.06 %
				Red	127.23	128.65	-1.12 %
				NIR	90.845	91.688	-0.93 %
			34%	Blue	108.04	107.29	0.69 %
				Green	97.263	96.883	0.39 %
				Red	81.465	81.362	0.13 %
				NIR	55.754	55.710	0.08 %
			22%	Blue	88.622	86.982	1.85 %
				Green	76.680	75.452	1.60 %
				Red	60.965	60.174	1.30 %
				NIR	39.454	38.998	1.16 %
			3.5%	Blue	39.209	38.418	2.02 %
				Green	27.305	26.649	2.40 %
				Red	16.809	16.322	2.90 %
				NIR	9.5891	9.2478	3.56 %
4/27/05	166 / 6	84 / 6	BL	Green	40.732	41.179	-1.10 %
				Red	20.992	21.554	-2.68 %
				NIR	132.03	130.32	1.30 %
				SWIR	11.251	11.314	-0.56 %
			DG	Green	162.37	161.79	0.36 %
				Red	183.29	182.68	0.33 %
				NIR	143.02	143.70	-0.48 %
				SWIR	40.295	40.198	0.24 %
			Perk	Green	179.29	175.62	2.05 %
				Red	195.10	191.54	1.82 %
				NIR	153.98	151.47	1.63 %
				SWIR	39.088	38.477	1.56 %

[1]Traditional Sun Photometer

[2]Novel Sun Photometer

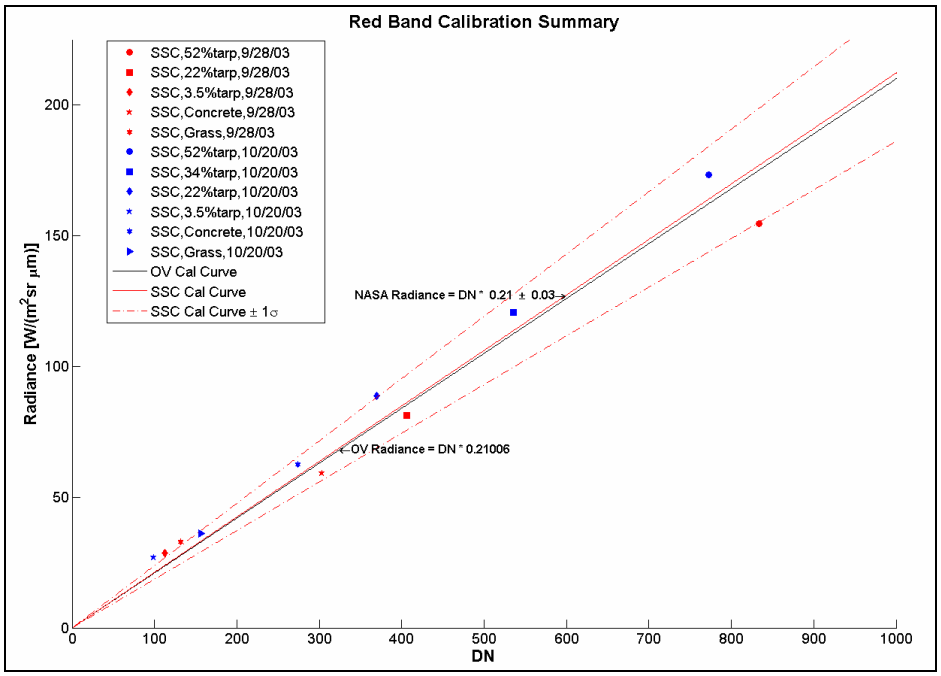

Figure 6. OrbView-3 radiometric characterization using traditional sun photometer data.

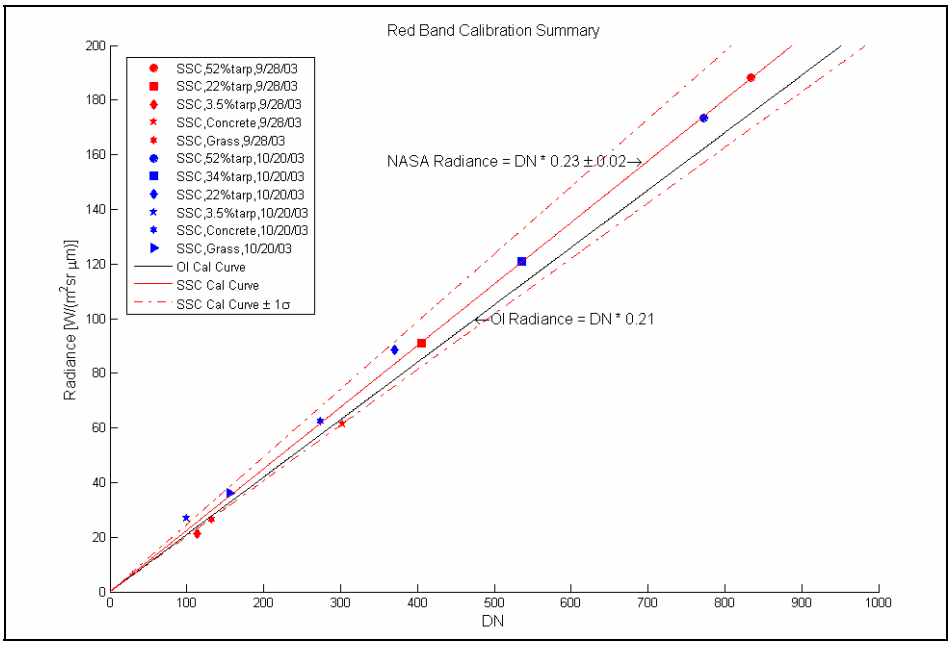

Figure 7. OrbView-3 radiometric characterization using novel sun photometer data.

The prototype calibration system, shown in Figure 8, consists of an 18" LabSphere integrating sphere fitted with a white LED (Luxeon V Portable DS40 LXHL-LW6C) in the back facing the internal baffle and a white LED, driven by a constant current source that utilizes photodiode feedback to maintain a desired light level. The photodiode (Hamamatsu S2592) was located in a side porthole near the front of the integrating sphere. Both the LED and photodiode are temperature stabilized to a temperature of 30 ºC using thermoelectric coolers. PID-1500s, made by Wavelength Electronics, are used to control the thermoelectric coolers. The photodiode has an internal thermistor and the LED has a 10 k ohm thermistor, which is inserted in a hole below the metal mounting plate of the LED, for temperature regulation. A schematic of the calibration system circuit design is shown in Appendix B.

Particular interest was focused on the development of a low noise constant current source to drive the LED. Batteries were selected as a low noise power source. In general, the system is comprised of low noise components including a photodiode, multiple operational amplifiers, and a voltage reference. As such, low noise components combined with temperature-stabilized components and a circuit design that allows feedback from the photodiode to stabilize the current through the LED produce this prototype of a portable field calibration system.

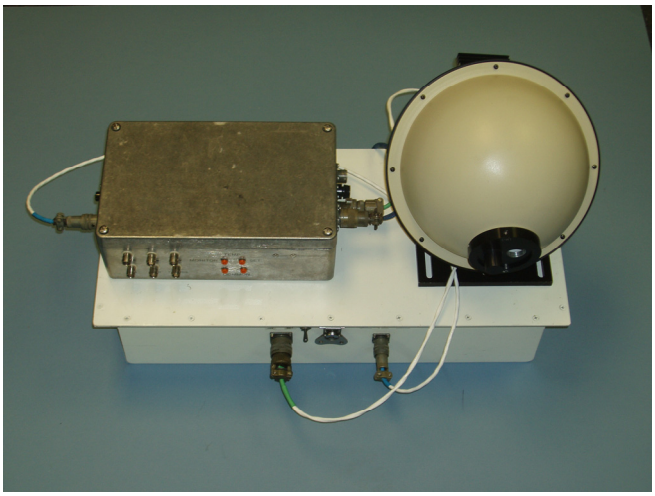

Figure 8. Novel sun photometer calibration system.

Successful testing of the prototype system was conducted in a laboratory environment which was typically about 25 ºC. A computer system with two NI-4351 data acquisition cards permit voltage monitoring of the constant current source circuit, temperature equivalent voltage monitoring from the PID-1500 controllers, and general power supply voltages. The calibration system was not field tested during this CDDF project. ASD V&V activities will support future field operation of this calibration system.

3.4 Conclusions

A novel sun photometer consisting of a calibrated spectroradiometer positioned over a 99 percent reflective Spectralon plaque was developed and tested in the field alongside traditional sun photometers. Atmospheric properties such as atmospheric optical depth, τ , and diffuse-to-global-ratio, D2G, that were obtained using the novel sun photometer compared favorably with that obtained from traditional sun photometers. With the exception of a single day, RMS values associated with differences in D2G ratios ranged from 0.006 to 0.02, and RMS values associated with aerosol optical depth differences ranged from 0.02 to 0.07. TOA radiance estimates that incorporate atmospheric data measurements made with the novel sun photometer, with the exception of a single day, also compared well with those obtained using traditional sun photometers, with percent differences ranging from .08 percent to 3.56 percent.

On the single day for which the traditional sun photometer data produced atmospheric parameters different from that produced with the novel sun photometer, data suggests that the novel sun photometer measurements were superior. The novel sun photometer was able to generate atmospheric parameters yielding TOA radiance values that agreed with subsequent day's data, unlike the traditional sun photometer. It is believed that this is due to the operational nature of the novel sun photometer. The novel sun photometer need only acquire data at the precise time the atmosphere is being characterized. In the case of a sensor characterization application, the novel sun photometer would only acquire data for a few minutes coincident with the sensor acquisition. Traditional sun photometers require several hours of data, so that on days with atmospheric variability, a traditional sun photometer actually yields results based on varying conditions that may not be present or valid at the time the atmosphere needs be characterized.

4.0 References

Berk, A., G. P. Anderson, P. K. Acharya, J. H. Chetwynd, L. S. Bernstein, E. P. Shettle, M. W. Matthew, and S. M. Adler-Golden, 2003. *MODTRAN4 Version 3 Revision 1 User's Manual.* Air Force Research Laboratory, Space Vehicles Directorate, Air Force Materiel Command, Hanscom AFB, MA, 11 February. 95 p. http://www.dodsbir.net/sitis/view_pdf.asp?id=BerkA00.pdf (accessed January 10, 2006).

Cornell University, 2003. Curious about astronomy? Ask an astronomer. Astronomy Department. http://curious.astro.cornell. edu/question.php?number=582 (accessed January 30, 2006).

Harrison, L., J. Michalsky, and J. Berndt, 1994. Automatic multifilter rotating shadow-band radiometer: An instrument for optical depth and radiation measurements. *Applied Optics* 33 (22): 5118–5125.

Harrison, L., and J. Michalsky, 1994. Objective algorithms for the retrieval of optical depths from ground-based measurements. *Applied Optics* 33 (22): 5126–5132.

Holben, B. N., V. Kalb, Y. J. Kaufman, D. Tanré, and E. Vermote, 1992. Aerosol retrieval over land from AVHRR data-application for atmospheric correction. *IEEE Transactions on Geoscience and Remote Sensing* 30: 212–222.

Jackson, R. D., T. R. Clarke, and M. S. Moran, 1992. Bidirectional calibration results for 11 spectralon and 16 BaSO4 reference reflectance panels. *Remote Sensing of Environment* 40 (3): 231–239.

Kasten, F., and A. T. Young, 1989. Revised optical air masses tables and approximation formula. *Applied Optics* 28 (22): 4738–4738.

O'Neill, N. T., and J. R. Miller, 1984. Combined solar aureole and solar beam extinction measurements. 1: Calibration considerations. *Applied Optics* 23 (20): 3691–3696.

Pagnutti, M., K. Holekamp, R. Ryan, S. Blonski, R. Sellers, B. Davis, and V. Zanoni, 2002. Measurement sets and sites commonly used for characterization. In *Proceedings of Integrated Remote Sensing at the Global, Regional and Local Scale: ISPRS Commission I Mid-Term Symposium*, November 8–15, Denver, CO, IAPRS, Vol. XXXIV, part 1. http://www.isprs.org/commission1/proceedings02/paper/MPagnutti_ISPRS2002.pdf (accessed January 30, 2006).

Pagnutti, M. A., R. E. Ryan, M. Kelly, K. Holekamp, V. Zanoni, K. Thome, and S. Schiller, 2003. Radiometric characterization of IKONOS multispectral imagery. *Remote Sensing of Environment* 88 (1-2): 53–68.

Reagan, J. A., L. W. Thomason, B. M. Herman, and J. M. Palmer, 1986. Assessment of atmospheric limitations on the determination of the solar spectral constant from ground spectroradiometer measurements. *IEEE Transactions on Geoscience and Remote Sensing* GE-24: 258–265.

Reagan, J. A., K. J. Thome, and B. M. Herman, 1992. A simple instrument and technique for measuring columnar water vapor via Near-IR differential solar transmission measurements. *IEEE Transactions on Geoscience and Remote Sensing* 30: 825–831.

Stern, D P., 2004. Deriving the astronomical unit. In From Stargazers to Starships, Chapter 12e. http://www-spof.gsfc.nasa.gov/stargaze/Svenus3.htm (accessed January 30, 2006).

U.S. Naval Observatory, 2003. Earth's seasons: Equinoxes, solstices, perihelion, and aphelion, 1992-2020. Astronomical Applications Department. http://aa.usno.navy.mil/data/docs/EarthSeasons.html (accessed January 30, 2006).

Zanoni, V., T. Stanley, R. Ryan, M. Pagnutti, B. Baldridge, S. Roylance, G. Snyder, and G. Lee, 2003. The Joint Agency Commercial Imagery Evaluation (JACIE) team: Overview and IKONOS joint characterization approach. *Remote Sensing of Environment* 88 (1-2): 17–22.

This page intentionally blank

Appendix A. Novel Sun Photometer (NSP) Results

A.1. Results for September 17, 2003

A.1.1. Optical Depth, ASR 27

	SSC 9/17/03 – 16:30 GMT			
	ASR 27	NSP	Difference	Percent Difference
Band	Generated	Generated	ASR-NSP	1 - (NSP/ASR)
380 nm	0.529	0.6475	-0.118	-22.39%
400 nm	0.442	0.5632	-0.121	-27.43%
440 nm	0.315	0.3673	-0.052	-16.60%
520 nm	0.183	0.2413	-0.058	-31.88%
610 nm	0.134	0.1506	-0.017	-12.42%
670 nm	0.083	0.0960	-0.013	-15.65%
780 nm	0.052	0.0420	0.010	19.21%
870 nm	0.031	-0.0049	0.036	115.80%
		RMS 1:8	0.068	
	SSC 9/17/03 – 16:38 GMT			
	ASR 27	NSP	Difference	Percent Difference
Band	Generated	Generated	ASR-NSP	1 - (NSP/ASR)
380 nm	0.529	0.6601	-0.131	-24.78%
400 nm	0.442	0.5752	-0.133	-30.14%
440 nm	0.315	0.3795	-0.065	-20.49%
520 nm	0.183	0.2229	-0.040	-21.80%
610 nm	0.134	0.1596	-0.026	-19.14%
670 nm	0.083	0.1047	-0.022	-26.13%
780 nm	0.052	0.0505	0.001	2.88%
870 nm	0.031	0.0028	0.028	90.91%
		RMS 1:8	0.073	
	SSC 9/17/03 – 16:42 GMT			
	ASR 27	NSP	Difference	Percent Difference
Band	Generated	Generated	ASR-NSP	1 - (NSP/ASR)
380 nm	0.529	0.6435	-0.114	-21.64%
400 nm	0.442	0.5591	-0.117	-26.50%
440 nm	0.315	0.3641	-0.049	-15.58%
520 nm	0.183	0.2088	-0.026	-14.07%
610 nm	0.134	0.1461	-0.012	-8.99%
670 nm	0.083	0.0915	-0.008	-10.19%
780 nm	0.052	0.0370	0.015	28.94%
870 nm	0.031	-0.0112	0.042	136.09%
		RMS 1:8	0.063	

	SSC 9/17/03 – 16:52 GMT			
	ASR 27	NSP	Difference	Percent Difference
Band	Generated	Generated	ASR-NSP	1 - (NSP/ASR)
380 nm	0.529	0.6375	-0.109	-20.52%
400 nm	0.442	0.5545	-0.112	-25.45%
440 nm	0.315	0.3598	-0.045	-14.21%
520 nm	0.183	0.2053	-0.022	-12.18%
610 nm	0.134	0.1431	-0.009	-6.82%
670 nm	0.083	0.0888	-0.006	-6.95%
780 nm	0.052	0.0342	0.018	34.21%
870 nm	0.031	-0.0149	0.046	148.17%
		RMS 1:8	0.061	
	SSC 9/17/03 – 16:57 GMT			
	ASR 27	NSP	Difference	Percent Difference
Band	Generated	Generated	ASR-NSP	1 - (NSP/ASR)
380 nm	0.529	0.6399	-0.111	-20.97%
400 nm	0.442	0.5566	-0.115	-25.93%
440 nm	0.315	0.3607	-0.046	-14.52%
520 nm	0.183	0.2053	-0.022	-12.18%
610 nm	0.134	0.1420	-0.008	-6.00%
670 nm	0.083	0.0874	-0.004	-5.25%
780 nm	0.052	0.0318	0.020	38.75%
870 nm	0.031	-0.0172	0.048	155.63%
		RMS 1:8	0.062	

A.1.2. Optical Depth, MFRSR 451

	SSC 9/17/03 – 16:30 GMT			
	MFR 451	NSP	Difference	Percent Difference
Band	Generated	Generated	MFRSR-NSP	1 - (NSP/MFRSR)
415 nm	0.416	0.5095	-0.093	-22.47%
500 nm	0.228	0.2535	-0.026	-11.20%
615 nm	0.157	0.1481	0.009	5.69%
673 nm	0.101	0.0953	0.006	5.62%
870 nm	0.048	-0.0088	0.057	118.41%
		RMS 1:5	0.050	
	SSC 9/17/03 – 16:38 GMT			
	MFR 451	NSP	Difference	Percent Difference
Band	Generated	Generated	MFRSR-NSP	1 - (NSP/MFRSR)
415 nm	0.416	0.5210	-0.105	-25.23%
500 nm	0.228	0.2632	-0.035	-15.43%
615 nm	0.157	0.1571	0.000	-0.05%
673 nm	0.101	0.1039	-0.003	-2.91%
870 nm	0.048	-0.0010	0.049	102.04%
		RMS 1:5	0.054	

	SSC 9/17/03 – 16:42 GMT			
	MFR 451	NSP	Difference	Percent Difference
Band	Generated	Generated	MFRSR-NSP	1 - (NSP/MFRSR)
415 nm	0.416	0.5050	-0.089	-21.40%
500 nm	0.228	0.2487	-0.021	-9.08%
615 nm	0.157	0.1435	0.014	8.60%
673 nm	0.101	0.0907	0.010	10.20%
870 nm	0.048	-0.0149	0.063	131.13%
		RMS 1:5	0.050	

	SSC 9/17/03 – 16:52 GMT			
	MFR 451	NSP	Difference	Percent Difference
Band	Generated	Generated	MFRSR-NSP	1 - (NSP/MFRSR)
415 nm	0.416	0.5007	-0.085	-20.37%
500 nm	0.228	0.2455	-0.017	-7.66%
615 nm	0.157	0.1405	0.016	10.50%
673 nm	0.101	0.0880	0.013	12.91%
870 nm	0.048	-0.0186	0.067	138.71%
		RMS 1:5	0.050	

	SSC 9/17/03 – 16:57 GMT			
	MFR 451	NSP	Difference	Percent Difference
Band	Generated	Generated	MFRSR-NSP	1 - (NSP/MFRSR)
415 nm	0.416	0.5026	-0.087	-20.81%
500 nm	0.228	0.2457	-0.018	-7.77%
615 nm	0.157	0.1394	0.018	11.22%
673 nm	0.101	0.0866	0.014	14.27%
870 nm	0.048	-0.0211	0.069	143.93%
		RMS 1:5	0.051	

A.1.3. Optical Depth, MFRSR 477

	SSC 9/17/03 – 16:30 GMT			
	MFR 477	NSP	Difference	Percent Difference
Band	Generated	Generated	MFRSR-NSP	1 - (NSP/MFRSR)
415 nm	0.424	0.5062	-0.082	-19.40%
500 nm	0.233	0.2569	-0.024	-10.28%
615 nm	0.153	0.1493	0.004	2.42%
673 nm	0.101	0.0099	0.091	90.17%
870 nm	0.046	-0.0085	0.054	118.46%
		RMS 1:5	0.061	

	SSC 9/17/03 – 16:38 GMT			
	MFR 477	NSP	Difference	Percent Difference
Band	Generated	Generated	MFRSR-NSP	1 - (NSP/MFRSR)
415 nm	0.424	0.5177	-0.094	-22.10%
500 nm	0.233	0.2666	-0.034	-14.41%
615 nm	0.153	0.1583	-0.005	-3.49%
673 nm	0.101	0.1078	-0.007	-6.77%
870 nm	0.046	-0.0006	0.047	101.33%
		RMS 1:5	0.049	

	SSC 9/17/03 – 16:42 GMT			
	MFR 477	NSP	Difference	Percent Difference
Band	Generated	Generated	MFRSR-NSP	1 - (NSP/MFRSR)
415 nm	0.424	0.5018	-0.078	-18.34%
500 nm	0.233	0.2521	-0.019	-8.18%
615 nm	0.153	0.1447	0.008	5.40%
673 nm	0.101	0.0945	0.007	6.48%
870 nm	0.046	-0.0146	0.061	131.67%
		RMS 1:5	0.045	
	SSC 9/17/03 – 16:52 GMT			
	MFR 477	NSP	Difference	Percent Difference
Band	Generated	Generated	MFRSR-NSP	1 - (NSP/MFRSR)
415 nm	0.424	0.4974	-0.073	-17.31%
500 nm	0.233	0.2489	-0.016	-6.81%
615 nm	0.153	0.1418	0.011	7.35%
673 nm	0.101	0.0918	0.009	9.12%
870 nm	0.046	-0.0182	0.064	139.54%
		RMS 1:5	0.045	
	SSC 9/17/03 – 16:57 GMT			
	MFR 477	NSP	Difference	Percent Difference
Band	Generated	Generated	MFRSR-NSP	1 - (NSP/MFRSR)
415 nm	0.424	0.4992	-0.075	-17.74%
500 nm	0.233	0.2491	-0.016	-6.91%
615 nm	0.153	0.1406	0.012	8.08%
673 nm	0.101	0.0902	0.011	10.68%
870 nm	0.046	-0.0208	0.067	145.19%
		RMS 1:5	0.046	

A.1.4. Diffuse-to-Global Ratio, MFRSR 451

	SSC 9/17/03 – 16:30 GMT			
	MFR 451	NSP	Difference	Percent Difference
Band	Generated	Generated	MFRSR-NSP	1 - (NSP/MFRSR)
415 nm	0.2272	0.2136	0.014	5.97%
500 nm	0.1422	0.0926	0.050	34.86%
615 nm	0.0739	0.0141	0.060	80.99%
673 nm	0.0575	-0.0073	0.065	112.63%
870 nm	0.036	-0.0307	0.067	185.22%
		RMS 1:5	0.055	
	SSC 9/17/03 – 16:38 GMT			
	MFR 451	NSP	Difference	Percent Difference
Band	Generated	Generated	MFRSR-NSP	1 - (NSP/MFRSR)
415 nm	0.2276	0.2568	-0.029	-12.82%
500 nm	0.1431	0.1494	-0.006	-4.37%
615 nm	0.0747	0.0799	-0.005	-6.94%
673 nm	0.0583	0.0611	-0.003	-4.83%
870 nm	0.0366	0.0403	-0.004	-9.99%
		RMS 1:5	0.014	

	SSC 9/17/03 – 16:42 GMT			
	MFR 451	NSP	Difference	Percent Difference
Band	Generated	Generated	MFRSR-NSP	1 - (NSP/MFRSR)
415 nm	0.2279	0.2517	-0.024	-10.45%
500 nm	0.1436	0.1457	-0.002	-1.48%
615 nm	0.0751	0.0778	-0.003	-3.64%
673 nm	0.0586	0.0593	-0.001	-1.24%
870 nm	0.0369	0.0390	-0.002	-5.65%
		RMS 1:5	0.011	

	SSC 9/17/03 – 16:52 GMT			
	MFR 451	NSP	Difference	Percent Difference
Band	Generated	Generated	MFRSR-NSP	1 - (NSP/MFRSR)
415 nm	0.2279	0.2508	-0.023	-10.05%
500 nm	0.1445	0.1462	-0.002	-1.17%
615 nm	0.0758	0.0781	-0.002	-3.02%
673 nm	0.0592	0.0597	0.000	-0.80%
870 nm	0.0373	0.0386	-0.001	-3.42%
		RMS 1:5	0.010	

	SSC 9/17/03 – 16:57 GMT			
	MFR 451	NSP	Difference	Percent Difference
Band	Generated	Generated	MFRSR-NSP	1 - (NSP/MFRSR)
415 nm	0.2276	0.2506	-0.023	-10.10%
500 nm	0.1447	0.1457	-0.001	-0.68%
615 nm	0.076	0.0772	-0.001	-1.59%
673 nm	0.0593	0.0586	0.001	1.22%
870 nm	0.0375	0.0371	0.000	1.18%
		RMS 1:5	0.010	

A.1.5. Diffuse-to-Global Ratio, MFRSR 477

	SSC 9/17/03 – 16:30 GMT			
	MFR 477	NSP	Difference	Percent Difference
Band	Generated	Generated	MFRSR-NSP	1 - (NSP/MFRSR)
415 nm	0.2582	0.2139	0.044	17.15%
500 nm	0.1494	0.0937	0.056	37.26%
615 nm	0.0787	0.0144	0.064	81.64%
673 nm	0.06	-0.0090	0.069	114.98%
870 nm	0.0436	-0.0306	0.074	170.27%
		RMS 1:5	0.062	

	SSC 9/17/03 – 16:38 GMT			
	MFR 477	NSP	Difference	Percent Difference
Band	Generated	Generated	MFRSR-NSP	1 - (NSP/MFRSR)
415 nm	0.2578	0.2570	0.001	0.29%
500 nm	0.1496	0.1503	-0.001	-0.49%
615 nm	0.079	0.0802	-0.001	-1.55%
673 nm	0.0602	0.0596	0.001	1.07%
870 nm	0.0438	0.0403	0.004	8.01%
		RMS 1:5	0.002	

	SSC 9/17/03 – 16:42 GMT			
	MFR 477	NSP	Difference	Percent Difference
Band	Generated	Generated	MFRSR-NSP	1 - (NSP/MFRSR)
415 nm	0.2574	0.2520	0.005	2.11%
500 nm	0.1496	0.1467	0.003	1.96%
615 nm	0.079	0.0782	0.001	1.04%
673 nm	0.0602	0.0578	0.002	3.91%
870 nm	0.0438	0.0390	0.005	10.89%
		RMS 1:5	0.004	
	SSC 9/17/03 – 16:52 GMT			
	MFR 477	NSP	Difference	Percent Difference
Band	Generated	Generated	MFRSR-NSP	1 - (NSP/MFRSR)
415 nm	0.2557	0.2511	0.005	1.82%
500 nm	0.1486	0.1472	0.001	0.97%
615 nm	0.0785	0.0784	0.000	0.10%
673 nm	0.0598	0.0581	0.002	2.79%
870 nm	0.0436	0.0386	0.005	11.45%
		RMS 1:5	0.003	
	SSC 9/17/03 – 16:57 GMT			
	MFR 477	NSP	Difference	Percent Difference
Band	Generated	Generated	MFRSR-NSP	1 - (NSP/MFRSR)
415 nm	0.255	0.2508	0.004	1.63%
500 nm	0.1483	0.1466	0.002	1.12%
615 nm	0.0784	0.0776	0.001	1.08%
673 nm	0.0597	0.0569	0.003	4.62%
870 nm	0.0435	0.0371	0.006	14.78%
		RMS 1:5	0.004	

A.2. Results for September 28, 2003

A.2.1. Optical Depth, ASR 27

	SSC 9/28/03 – 16:41 GMT			
	ASR 27	NSP	Difference	Percent Difference
Band	Generated	Generated	ASR-NSP	1 - (NSP/ASR)
380 nm	1.003	0.6073	0.396	39.45%
400 nm	0.894	0.5288	0.365	40.85%
440 nm	0.736	0.3447	0.391	53.16%
520 nm	0.523	0.2031	0.320	61.16%
610 nm	0.399	0.1494	0.250	62.57%
670 nm	0.311	0.0993	0.212	68.06%
780 nm	0.233	0.0538	0.179	76.90%
870 nm	0.177	0.0107	0.166	93.98%
		RMS 1:8	0.298	

	SSC 9/28/03 – 16:42 GMT			
	ASR 27	NSP	Difference	Percent Difference
Band	Generated	Generated	ASR-NSP	1 - (NSP/ASR)
380 nm	1.003	0.5810	0.422	42.08%
400 nm	0.894	0.5042	0.390	43.60%
440 nm	0.736	0.3227	0.413	56.15%
520 nm	0.523	0.1848	0.338	64.66%
610 nm	0.399	0.1335	0.266	66.55%
670 nm	0.311	0.0850	0.226	72.67%
780 nm	0.233	0.0411	0.192	82.35%
870 nm	0.177	-0.0012	0.178	100.65%
		RMS 1:8	0.317	

A.2.2. Optical Depth, MFRSR 451

	SSC 9/28/03 – 16:41 GMT			
	MFR 451	NSP	Difference	Percent Difference
Band	Generated	Generated	MFRSR-NSP	1 - (NSP/MFRSR)
415 nm	1.318	0.4775	0.841	63.77%
500 nm	0.686	0.2392	0.447	65.14%
615 nm	0.529	0.1462	0.383	72.36%
673 nm	0.44	0.0993	0.341	77.44%
870 nm	0.3	0.0068	0.293	97.72%
		RMS 1:5	0.501	

	SSC 9/28/03 – 16:42 GMT			
	MFR 451	NSP	Difference	Percent Difference
Band	Generated	Generated	MFRSR-NSP	1 - (NSP/MFRSR)
415 nm	1.318	0.4538	0.864	65.57%
500 nm	0.686	0.2199	0.466	67.94%
615 nm	0.529	0.1304	0.399	75.35%
673 nm	0.44	0.0850	0.355	80.68%
870 nm	0.3	-0.0051	0.305	101.70%
		RMS 1:5	0.518	

A.2.3. Optical Depth, MFRSR 477

	SSC 9/28/03 – 16:41 GMT			
	MFR 477	NSP	Difference	Percent Difference
Band	Generated	Generated	MFRSR-NSP	1 - (NSP/MFRSR)
415 nm	0.893	0.4743	0.419	46.89%
500 nm	0.623	0.2424	0.381	61.10%
615 nm	0.433	0.1474	0.286	65.96%
673 nm	0.344	0.1056	0.238	69.29%
870 nm	0.204	0.0072	0.197	96.45%
		RMS 1:5	0.315	

	SSC 9/28/03 – 16:42 GMT			
	MFR 477	NSP	Difference	Percent Difference
Band	Generated	Generated	MFRSR-NSP	1 - (NSP/MFRSR)
415 nm	0.893	0.4506	0.442	49.54%
500 nm	0.623	0.2231	0.400	64.19%
615 nm	0.433	0.1316	0.301	69.61%
673 nm	0.344	0.0911	0.253	73.51%
870 nm	0.204	-0.0047	0.209	102.31%
		RMS 1:5	0.333	

A.2.4. Diffuse-to-Global Ratio, MFRSR 451

	SSC 9/28/03 – 16:41 GMT			
	MFR 451	NSP	Difference	Percent Difference
Band	Generated	Generated	MFRSR-NSP	1 - (NSP/MFRSR)
415 nm	0	0.2495	-0.250	#DIV/0!
500 nm	0.1368	0.1468	-0.010	-7.28%
615 nm	0.0757	0.0830	-0.007	-9.65%
673 nm	0.0592	0.0661	-0.007	-11.62%
870 nm	0.0384	0.0474	-0.009	-23.51%
		RMS 1:5	0.112	

	SSC 9/28/03 – 16:42 GMT			
	MFR 451	NSP	Difference	Percent Difference
Band	Generated	Generated	MFRSR-NSP	1 - (NSP/MFRSR)
415 nm	0	0.2340	-0.234	#DIV/0!
500 nm	0.1358	0.1340	0.002	1.31%
615 nm	0.0751	0.0739	0.001	1.57%
673 nm	0.0587	0.0583	0.000	0.67%
870 nm	0.038	0.0429	-0.005	-12.82%
		RMS 1:5	0.105	

A.2.5. Diffuse-to-Global Ratio, MFRSR 477

	SSC 9/28/03 – 16:41 GMT			
	MFR 477	NSP	Difference	Percent Difference
Band	Generated	Generated	MFRSR-NSP	1 - (NSP/MFRSR)
415 nm	0.2454	0.2498	-0.004	-1.78%
500 nm	0.144	0.1477	-0.004	-2.56%
615 nm	0.0809	0.0833	-0.002	-2.97%
673 nm	0.0645	0.0648	0.000	-0.40%
870 nm	0.0509	0.0474	0.003	6.80%
		RMS 1:5	0.003	

	SSC 9/28/03 – 16:42 GMT			
	MFR 477	NSP	Difference	Percent Difference
Band	Generated	Generated	MFRSR-NSP	1 - (NSP/MFRSR)
415 nm	0.2444	0.2343	0.010	4.14%
500 nm	0.1431	0.1349	0.008	5.73%
615 nm	0.0803	0.0742	0.006	7.59%
673 nm	0.0639	0.0567	0.007	11.33%
870 nm	0.0506	0.0429	0.008	15.23%
		RMS 1:5	0.008	

A.3. Results for January 10, 2004

A.3.1. Optical Depth, ASR 27

	SSC 1/10/04 – 16:13 GMT			
	ASR 27	NSP	Difference	Percent Difference
Band	Generated	Generated	ASR-NSP	1 - (NSP/ASR)
380 nm	0.588	0.6009	-0.013	-2.20%
400 nm	0.495	0.4890	0.006	1.21%
440 nm	0.366	0.3273	0.039	10.57%
520 nm	0.224	0.2030	0.021	9.38%
610 nm	0.161	0.1592	0.002	1.13%
670 nm	0.108	0.1033	0.005	4.40%
780 nm	0.07	0.0724	-0.002	-3.50%
870 nm	0.049	0.0544	-0.005	-11.07%
		RMS 1:8	0.017	

	SSC 1/10/04 – 16:33 GMT			
	ASR 27	NSP	Difference	Percent Difference
Band	Generated	Generated	ASR-NSP	1 - (NSP/ASR)
380 nm	0.588	0.5982	-0.010	-1.74%
400 nm	0.495	0.4852	0.010	1.99%
440 nm	0.366	0.3216	0.044	12.14%
520 nm	0.224	0.1988	0.025	11.25%
610 nm	0.161	0.1563	0.005	2.91%
670 nm	0.108	0.1002	0.008	7.26%
780 nm	0.07	0.0691	0.001	1.33%
870 nm	0.049	0.0508	-0.002	-3.58%
		RMS 1:8	0.019	

A.3.2. Optical Depth, MFRSR 477

	SSC 1/10/04 – 16:13 GMT			
	MFR 477	NSP	Difference	Percent Difference
Band	Generated	Generated	MFRSR-NSP	1 - (NSP/MFRSR)
415 nm	0.477	0.4493	0.028	5.82%
500 nm	0.284	0.2451	0.039	13.68%
615 nm	0.179	0.1515	0.027	15.35%
673 nm	0.128	0.1036	0.024	19.08%
870 nm	0.065	0.0517	0.013	20.42%
		RMS 1:5	0.028	

	SSC 1/10/04 – 16:33 GMT			
	MFR 477	NSP	Difference	Percent Difference
Band	Generated	Generated	MFRSR-NSP	1 - (NSP/MFRSR)
415 nm	0.477	0.4459	0.031	6.52%
500 nm	0.284	0.2415	0.042	14.96%
615 nm	0.179	0.1485	0.030	17.03%
673 nm	0.128	0.1007	0.027	21.36%
870 nm	0.065	0.0479	0.017	26.27%
		RMS 1:5	0.031	

A.3.3. Diffuse-to-Global Ratio, MFRSR 477

	SSC 1/10/04 – 16:13 GMT			
	MFR 477	NSP	Difference	Percent Difference
Band	Generated	Generated	MFRSR-NSP	1 - (NSP/MFRSR)
415 nm	0.4105	0.4239	-0.013	-3.26%
500 nm	0.2574	0.2715	-0.014	-5.48%
615 nm	0.1434	0.1597	-0.016	-11.37%
673 nm	0.1186	0.1244	-0.006	-4.86%
870 nm	0.0745	0.0796	-0.005	-6.82%
		RMS 1:5	0.012	

	SSC 1/10/04 – 16:33 GMT			
	MFR 477	NSP	Difference	Percent Difference
Band	Generated	Generated	MFRSR-NSP	1 - (NSP/MFRSR)
415 nm	0.3935	0.3881	0.005	1.37%
500 nm	0.2469	0.2404	0.007	2.63%
615 nm	0.1428	0.1365	0.006	4.41%
673 nm	0.1141	0.1044	0.010	8.51%
870 nm	0.0722	0.0664	0.006	8.00%
		RMS 1:5	0.007	

A.4. Results for December 15, 2004

A.4.1. Optical Depth, ASR 25

	SSC 12/15/04 – 16:23 GMT			
	ASR 25	NSP	Difference	Percent Difference
Band	Generated	Generated	ASR-NSP	1 - (NSP/ASR)
380 nm	0.501	0.4653	0.036	7.13%
400 nm	0.416	0.4473	-0.031	-7.52%
440 nm	0.295	0.2983	-0.003	-1.13%
520 nm	0.171	0.1519	0.019	11.18%
610 nm	0.121	0.1125	0.008	7.02%
670 nm	0.078	0.0712	0.007	8.77%
780 nm	0.042	0.0494	-0.007	-17.65%
870 nm	0.031	0.0467	-0.016	-50.68%
		RMS 1:8	0.020	

	SSC 12/15/04 – 16:30 GMT			
	ASR 25	NSP	Difference	Percent Difference
Band	Generated	Generated	ASR-NSP	1 - (NSP/ASR)
380 nm	0.501	0.4546	0.046	9.26%
400 nm	0.416	0.4380	-0.022	-5.29%
440 nm	0.295	0.2888	0.006	2.09%
520 nm	0.171	0.1431	0.028	16.33%
610 nm	0.121	0.1042	0.017	13.86%
670 nm	0.078	0.0631	0.015	19.04%
780 nm	0.042	0.0421	0.000	-0.19%
870 nm	0.031	0.0400	-0.009	-28.97%
		RMS 1:8	0.022	

	SSC 12/15/04 – 16:45 GMT			
	ASR 25	NSP	Difference	Percent Difference
Band	Generated	Generated	ASR-NSP	1 - (NSP/ASR)
380 nm	0.501	0.4575	0.043	8.68%
400 nm	0.416	0.4423	-0.026	-6.33%
440 nm	0.295	0.2911	0.004	1.33%
520 nm	0.171	0.1446	0.026	15.43%
610 nm	0.121	0.1058	0.015	12.56%
670 nm	0.078	0.0647	0.013	17.04%
780 nm	0.042	0.0432	-0.001	-2.95%
870 nm	0.031	0.0417	-0.011	-34.63%
		RMS 1:8	0.022	

	SSC 12/15/04 – 17:00 GMT			
	ASR 25	NSP	Difference	Percent Difference
Band	Generated	Generated	ASR-NSP	1 - (NSP/ASR)
380 nm	0.501	0.4543	0.047	9.33%
400 nm	0.416	0.4400	-0.024	-5.76%
440 nm	0.295	0.2870	0.008	2.71%
520 nm	0.171	0.1408	0.030	17.68%
610 nm	0.121	0.1024	0.019	15.39%
670 nm	0.078	0.0613	0.017	21.35%
780 nm	0.042	0.0402	0.002	4.20%
870 nm	0.031	0.0387	-0.008	-24.91%
		RMS 1:8	0.024	

	SSC 12/15/04 – 17:14 GMT			
	ASR 25	NSP	Difference	Percent Difference
Band	Generated	Generated	ASR-NSP	1 - (NSP/ASR)
380 nm	0.501	0.4509	0.050	10.01%
400 nm	0.416	0.4381	-0.022	-5.30%
440 nm	0.295	0.2849	0.010	3.41%
520 nm	0.171	0.1391	0.032	18.63%
610 nm	0.121	0.1014	0.020	16.18%
670 nm	0.078	0.0606	0.017	22.28%
780 nm	0.042	0.0398	0.002	5.16%
870 nm	0.031	0.0378	-0.007	-21.96%
		RMS 1:8	0.025	

	SSC 12/15/04 – 17:30 GMT			
	ASR 25	NSP	Difference	Percent Difference
Band	Generated	Generated	ASR-NSP	1 - (NSP/ASR)
380 nm	0.501	0.4534	0.048	9.50%
400 nm	0.416	0.4411	-0.025	-6.02%
440 nm	0.295	0.2868	0.008	2.79%
520 nm	0.171	0.1405	0.030	17.82%
610 nm	0.121	0.1025	0.018	15.25%
670 nm	0.078	0.0616	0.016	21.07%
780 nm	0.042	0.0404	0.002	3.90%
870 nm	0.031	0.0380	-0.007	-22.50%
		RMS 1:8	0.024	

A.4.2. Optical Depth, ASR 27

	SSC 12/15/04 – 16:23 GMT			
	ASR 27	NSP	Difference	Percent Difference
Band	Generated	Generated	ASR-NSP	1 - (NSP/ASR)
380 nm	0.493	0.4868	0.006	1.26%
400 nm	0.413	0.4365	-0.023	-5.69%
440 nm	0.295	0.2686	0.026	8.95%
520 nm	0.171	0.1497	0.021	12.44%
610 nm	0.121	0.1151	0.006	4.88%
670 nm	0.077	0.0720	0.005	6.54%
780 nm	0.045	0.0496	-0.005	-10.20%
870 nm	0.03	0.0469	-0.017	-56.35%
		RMS 1:8	0.016	

	SSC 12/15/04 – 16:30 GMT			
	ASR 27	NSP	Difference	Percent Difference
Band	Generated	Generated	ASR-NSP	1 - (NSP/ASR)
380 nm	0.493	0.4764	0.017	3.37%
400 nm	0.413	0.4272	-0.014	-3.44%
440 nm	0.295	0.2591	0.036	12.18%
520 nm	0.171	0.1408	0.030	17.66%
610 nm	0.121	0.1069	0.014	11.69%
670 nm	0.077	0.0639	0.013	16.95%
780 nm	0.045	0.0422	0.003	6.12%
870 nm	0.03	0.0401	-0.010	-33.68%
		RMS 1:8	0.020	

	SSC 12/15/04 – 16:45 GMT			
	ASR 27	NSP	Difference	Percent Difference
Band	Generated	Generated	ASR-NSP	1 - (NSP/ASR)
380 nm	0.493	0.4799	0.013	2.65%
400 nm	0.413	0.4313	-0.018	-4.44%
440 nm	0.295	0.2609	0.034	11.56%
520 nm	0.171	0.1422	0.029	16.86%
610 nm	0.121	0.1085	0.013	10.34%
670 nm	0.077	0.0655	0.012	14.95%
780 nm	0.045	0.0434	0.002	3.54%
870 nm	0.03	0.0419	-0.012	-39.63%
		RMS 1:8	0.019	

	SSC 12/15/04 – 17:00 GMT			
	ASR 27	NSP	Difference	Percent Difference
Band	Generated	Generated	ASR-NSP	1 - (NSP/ASR)
380 nm	0.493	0.4772	0.016	3.21%
400 nm	0.413	0.4288	-0.016	-3.84%
440 nm	0.295	0.2565	0.038	13.05%
520 nm	0.171	0.1383	0.033	19.13%
610 nm	0.121	0.1051	0.016	13.13%
670 nm	0.077	0.0621	0.015	19.35%
780 nm	0.045	0.0403	0.005	10.36%
870 nm	0.03	0.0389	-0.009	-29.68%
		RMS 1:8	0.021	

	SSC 12/15/04 – 17:14 GMT			
	ASR 27	NSP	Difference	Percent Difference
Band	Generated	Generated	ASR-NSP	1 - (NSP/ASR)
380 nm	0.493	0.4741	0.019	3.83%
400 nm	0.413	0.4269	-0.014	-3.38%
440 nm	0.295	0.2544	0.041	13.76%
520 nm	0.171	0.1366	0.034	20.12%
610 nm	0.121	0.1042	0.017	13.92%
670 nm	0.077	0.0614	0.016	20.29%
780 nm	0.045	0.0400	0.005	11.19%
870 nm	0.03	0.0380	-0.008	-26.65%
		RMS 1:8	0.022	
	SSC 12/15/04 – 17:30 GMT			
	ASR 27	NSP	Difference	Percent Difference
Band	Generated	Generated	ASR-NSP	1 - (NSP/ASR)
380 nm	0.493	0.4770	0.016	3.25%
400 nm	0.413	0.4299	-0.017	-4.08%
440 nm	0.295	0.2560	0.039	13.22%
520 nm	0.171	0.1379	0.033	19.37%
610 nm	0.121	0.1053	0.016	12.95%
670 nm	0.077	0.0624	0.015	19.00%
780 nm	0.045	0.0405	0.004	9.99%
870 nm	0.03	0.0382	-0.008	-27.29%
		RMS 1:8	0.022	

A.4.3. Optical Depth, MFRSR 451

	SSC 12/15/04 – 16:23 GMT			
	MFR 451	NSP	Difference	Percent Difference
Band	Generated	Generated	MFRSR-NSP	1 - (NSP/MFRSR)
415 nm	0.394	0.3747	0.019	4.90%
500 nm	0.216	0.1861	0.030	13.83%
615 nm	0.137	0.1081	0.029	21.07%
673 nm	0.088	0.0711	0.017	19.25%
870 nm	0.04	0.0444	-0.004	-10.90%
		RMS 1:5	0.022	
	SSC 12/15/04 – 16:30 GMT			
	MFR 451	NSP	Difference	Percent Difference
Band	Generated	Generated	MFRSR-NSP	1 - (NSP/MFRSR)
415 nm	0.394	0.3653	0.029	7.29%
500 nm	0.216	0.1773	0.039	17.92%
615 nm	0.137	0.0998	0.037	27.16%
673 nm	0.088	0.0631	0.025	28.34%
870 nm	0.04	0.0378	0.002	5.61%
		RMS 1:5	0.029	

	SSC 12/15/04 – 16:45 GMT			
	MFR 451	NSP	Difference	Percent Difference
Band	Generated	Generated	MFRSR-NSP	1 - (NSP/MFRSR)
415 nm	0.394	0.3685	0.026	6.48%
500 nm	0.216	0.1792	0.037	17.06%
615 nm	0.137	0.1013	0.036	26.08%
673 nm	0.088	0.0646	0.023	26.55%
870 nm	0.04	0.0394	0.001	1.51%
		RMS 1:5	0.028	
	SSC 12/15/04 – 17:00 GMT			
	MFR 451	NSP	Difference	Percent Difference
Band	Generated	Generated	MFRSR-NSP	1 - (NSP/MFRSR)
415 nm	0.394	0.3651	0.029	7.32%
500 nm	0.216	0.1754	0.041	18.78%
615 nm	0.137	0.0978	0.039	28.60%
673 nm	0.088	0.0613	0.027	30.36%
870 nm	0.04	0.0362	0.004	9.59%
		RMS 1:5	0.031	
	SSC 12/15/04 – 17:14 GMT			
	MFR 451	NSP	Difference	Percent Difference
Band	Generated	Generated	MFRSR-NSP	1 - (NSP/MFRSR)
415 nm	0.394	0.3632	0.031	7.80%
500 nm	0.216	0.1740	0.042	19.43%
615 nm	0.137	0.0968	0.040	29.31%
673 nm	0.088	0.0606	0.027	31.17%
870 nm	0.04	0.0353	0.005	11.68%
		RMS 1:5	0.032	
	SSC 12/15/04 – 17:30 GMT			
	MFR 451	NSP	Difference	Percent Difference
Band	Generated	Generated	MFRSR-NSP	1 - (NSP/MFRSR)
415 nm	0.394	0.3657	0.028	7.18%
500 nm	0.216	0.1756	0.040	18.71%
615 nm	0.137	0.0979	0.039	28.54%
673 nm	0.088	0.0615	0.026	30.09%
870 nm	0.04	0.0355	0.005	11.29%
		RMS 1:5	0.031	

A.4.4. Optical Depth, MFRSR 477

	SSC 12/15/04 – 16:23 GMT			
	MFR 477	NSP	Difference	Percent Difference
Band	Generated	Generated	MFRSR-NSP	1 - (NSP/MFRSR)
415 nm	0.429	0.3730	0.056	13.05%
500 nm	0.244	0.1883	0.056	22.81%
615 nm	0.155	0.1097	0.045	29.26%
673 nm	0.109	0.0703	0.039	35.49%
870 nm	0.058	0.0444	0.014	23.40%
		RMS 1:5	0.045	

	SSC 12/15/04 – 16:30 GMT			
	MFR 477	NSP	Difference	Percent Difference
Band	Generated	Generated	MFRSR-NSP	1 - (NSP/MFRSR)
415 nm	0.429	0.3636	0.065	15.25%
500 nm	0.244	0.1795	0.065	26.44%
615 nm	0.155	0.1013	0.054	34.64%
673 nm	0.109	0.0623	0.047	42.83%
870 nm	0.058	0.0378	0.020	34.81%
		RMS 1:5	0.053	

	SSC 12/15/04 – 16:45 GMT			
	MFR 477	NSP	Difference	Percent Difference
Band	Generated	Generated	MFRSR-NSP	1 - (NSP/MFRSR)
415 nm	0.429	0.3667	0.062	14.52%
500 nm	0.244	0.1814	0.063	25.65%
615 nm	0.155	0.1028	0.052	33.66%
673 nm	0.109	0.0639	0.045	41.37%
870 nm	0.058	0.0394	0.019	31.99%
		RMS 1:5	0.051	

	SSC 12/15/04 – 17:00 GMT			
	MFR 477	NSP	Difference	Percent Difference
Band	Generated	Generated	MFRSR-NSP	1 - (NSP/MFRSR)
415 nm	0.429	0.3633	0.066	15.31%
500 nm	0.244	0.1777	0.066	27.17%
615 nm	0.155	0.0994	0.056	35.88%
673 nm	0.109	0.0605	0.049	44.51%
870 nm	0.058	0.0362	0.022	37.59%
		RMS 1:5	0.054	

	SSC 12/15/04 – 17:14 GMT			
	MFR 477	NSP	Difference	Percent Difference
Band	Generated	Generated	MFRSR-NSP	1 - (NSP/MFRSR)
415 nm	0.429	0.3614	0.068	15.76%
500 nm	0.244	0.1763	0.068	27.75%
615 nm	0.155	0.0984	0.057	36.50%
673 nm	0.109	0.0598	0.049	45.14%
870 nm	0.058	0.0354	0.023	38.98%
		RMS 1:5	0.055	

	SSC 12/15/04 – 17:30 GMT			
	MFR 477	NSP	Difference	Percent Difference
Band	Generated	Generated	MFRSR-NSP	1 - (NSP/MFRSR)
415 nm	0.429	0.3638	0.065	15.19%
500 nm	0.244	0.1779	0.066	27.10%
615 nm	0.155	0.0995	0.055	35.80%
673 nm	0.109	0.0608	0.048	44.21%
870 nm	0.058	0.0356	0.022	38.70%
		RMS 1:5	0.054	

A.4.5. Diffuse-to-Global Ratio, MFRSR 451

	SSC 12/15/04 – 16:23 GMT			
	MFR 451	NSP	Difference	Percent Difference
Band	Generated	Generated	MFRSR-NSP	1 - (NSP/MFRSR)
415 nm	0.3133	0.3293	-0.016	-5.12%
500 nm	0.1739	0.1891	-0.015	-8.73%
615 nm	0.0861	0.1056	-0.019	-22.65%
673 nm	0.067	0.0844	-0.017	-25.97%
870 nm	0.0403	0.0580	-0.018	-43.93%
		RMS 1:5	0.017	

	SSC 12/15/04 – 16:30 GMT			
	MFR 451	NSP	Difference	Percent Difference
Band	Generated	Generated	MFRSR-NSP	1 - (NSP/MFRSR)
415 nm	0.3083	0.3140	-0.006	-1.84%
500 nm	0.1711	0.1748	-0.004	-2.14%
615 nm	0.0847	0.0921	-0.007	-8.78%
673 nm	0.066	0.0712	-0.005	-7.91%
870 nm	0.04	0.0456	-0.006	-13.94%
		RMS 1:5	0.006	

	SSC 12/15/04 – 16:45 GMT			
	MFR 451	NSP	Difference	Percent Difference
Band	Generated	Generated	MFRSR-NSP	1 - (NSP/MFRSR)
415 nm	0.3001	0.3071	-0.007	-2.32%
500 nm	0.1669	0.1716	-0.005	-2.80%
615 nm	0.0831	0.0913	-0.008	-9.91%
673 nm	0.0646	0.0710	-0.006	-9.84%
870 nm	0.0395	0.0456	-0.006	-15.39%
		RMS 1:5	0.007	

	SSC 12/15/04 – 17:00 GMT			
	MFR 451	NSP	Difference	Percent Difference
Band	Generated	Generated	MFRSR-NSP	1 - (NSP/MFRSR)
415 nm	0.291	0.2982	-0.007	-2.48%
500 nm	0.1617	0.1658	-0.004	-2.56%
615 nm	0.08	0.0880	-0.008	-9.97%
673 nm	0.0625	0.0680	-0.005	-8.79%
870 nm	0.0385	0.0438	-0.005	-13.66%
		RMS 1:5	0.006	

	SSC 12/15/04 – 17:14 GMT			
	MFR 451	NSP	Difference	Percent Difference
Band	Generated	Generated	MFRSR-NSP	1 - (NSP/MFRSR)
415 nm	0.284	0.2925	-0.009	-2.99%
500 nm	0.1576	0.1628	-0.005	-3.29%
615 nm	0.0776	0.0869	-0.009	-11.98%
673 nm	0.0606	0.0674	-0.007	-11.28%
870 nm	0.0379	0.0433	-0.005	-14.13%
		RMS 1:5	0.007	

	SSC 12/15/04 – 17:30 GMT			
	MFR 451	NSP	Difference	Percent Difference
Band	Generated	Generated	MFRSR-NSP	1 - (NSP/MFRSR)
415 nm	0.2798	0.2893	-0.010	-3.40%
500 nm	0.1556	0.1609	-0.005	-3.38%
615 nm	0.0767	0.0858	-0.009	-11.82%
673 nm	0.0599	0.0666	-0.007	-11.17%
870 nm	0.0375	0.0434	-0.006	-15.61%
		RMS 1:5	0.007	

A.4.6. Diffuse-to-Global Ratio, MFRSR 477

	SSC 12/15/04 – 16:23 GMT			
	MFR 477	NSP	Difference	Percent Difference
Band	Generated	Generated	MFRSR-NSP	1 - (NSP/MFRSR)
415 nm	0.3143	0.3296	-0.015	-4.88%
500 nm	0.1746	0.1903	-0.016	-9.01%
615 nm	0.09	0.1059	-0.016	-17.67%
673 nm	0.0687	0.0826	-0.014	-20.25%
870 nm	0.0477	0.0580	-0.010	-21.69%
		RMS 1:5	0.014	

	SSC 12/15/04 – 16:30 GMT			
	MFR 477	NSP	Difference	Percent Difference
Band	Generated	Generated	MFRSR-NSP	1 - (NSP/MFRSR)
415 nm	0.3091	0.3143	-0.005	-1.68%
500 nm	0.1715	0.1760	-0.005	-2.63%
615 nm	0.0884	0.0924	-0.004	-4.56%
673 nm	0.0675	0.0695	-0.002	-2.96%
870 nm	0.0473	0.0456	0.002	3.53%
		RMS 1:5	0.004	

	SSC 12/15/04 – 16:45 GMT			
	MFR 477	NSP	Difference	Percent Difference
Band	Generated	Generated	MFRSR-NSP	1 - (NSP/MFRSR)
415 nm	0.2995	0.3074	-0.008	-2.63%
500 nm	0.1661	0.1728	-0.007	-4.01%
615 nm	0.0853	0.0916	-0.006	-7.44%
673 nm	0.0655	0.0693	-0.004	-5.75%
870 nm	0.0466	0.0456	0.001	2.12%
		RMS 1:5	0.006	

	SSC 12/15/04 – 17:00 GMT			
	MFR 477	NSP	Difference	Percent Difference
Band	Generated	Generated	MFRSR-NSP	1 - (NSP/MFRSR)
415 nm	0.2917	0.2985	-0.007	-2.33%
500 nm	0.1615	0.1670	-0.005	-3.39%
615 nm	0.0829	0.0883	-0.005	-6.47%
673 nm	0.0637	0.0664	-0.003	-4.30%
870 nm	0.0463	0.0438	0.003	5.44%
		RMS 1:5	0.005	

	SSC 12/15/04 – 17:14 GMT			
	MFR 477	NSP	Difference	Percent Difference
Band	Generated	Generated	MFRSR-NSP	1 - (NSP/MFRSR)
415 nm	0.2872	0.2928	-0.006	-1.95%
500 nm	0.1588	0.1639	-0.005	-3.23%
615 nm	0.0818	0.0872	-0.005	-6.56%
673 nm	0.0628	0.0658	-0.003	-4.84%
870 nm	0.0461	0.0433	0.003	6.00%
		RMS 1:5	0.005	

	SSC 12/15/04 – 17:30 GMT			
	MFR 477	NSP	Difference	Percent Difference
Band	Generated	Generated	MFRSR-NSP	1 - (NSP/MFRSR)
415 nm	0.2837	0.2896	-0.006	-2.08%
500 nm	0.1568	0.1620	-0.005	-3.31%
615 nm	0.0809	0.0861	-0.005	-6.37%
673 nm	0.0623	0.0651	-0.003	-4.55%
870 nm	0.0458	0.0434	0.002	5.27%
		RMS 1:5	0.005	

A.5. Results for April 27, 2005

A.5.1. Optical Depth, ASR 26

	Wiggins 4/27/05 – 16:30			
	ASR 26	NSP	Difference	Percent Difference
Band	Generated	Generated	ASR-NSP	1 - (NSP/ASR)
380 nm	0.525	0.5740	-0.049	-9.32%
400 nm	0.417	0.6005	-0.183	-44.00%
440 nm	0.316	0.3342	-0.018	-5.75%
520 nm	0.208	0.2171	-0.009	-4.39%
610 nm	0.149	0.1816	-0.033	-21.89%
670 nm	0.097	0.1334	-0.036	-37.51%
780 nm	0.06	0.0952	-0.035	-58.66%
870 nm	0.054	0.0822	-0.028	-52.22%
		RMS 1:8	0.071	

	Wiggins 4/27/05 – 16:40			
	ASR 26	NSP	Difference	Percent Difference
Band	Generated	Generated	ASR-NSP	1 - (NSP/ASR)
380 nm	0.525	0.5753	-0.050	-9.58%
400 nm	0.417	0.6036	-0.187	-44.75%
440 nm	0.316	0.3355	-0.020	-6.18%
520 nm	0.208	0.2180	-0.010	-4.83%
610 nm	0.149	0.1822	-0.033	-22.27%
670 nm	0.097	0.1338	-0.037	-37.99%
780 nm	0.06	0.0944	-0.034	-57.37%
870 nm	0.054	0.0807	-0.027	-49.38%
		RMS 1:8	0.073	

	Wiggins 4/27/05 – 16:50			
	ASR 26	NSP	Difference	Percent Difference
Band	Generated	Generated	ASR-NSP	1 - (NSP/ASR)
380 nm	0.525	0.5700	-0.045	-8.57%
400 nm	0.417	0.6011	-0.184	-44.16%
440 nm	0.316	0.3332	-0.017	-5.44%
520 nm	0.208	0.2167	-0.009	-4.19%
610 nm	0.149	0.1818	-0.033	-22.03%
670 nm	0.097	0.1335	-0.037	-37.66%
780 nm	0.06	0.0950	-0.035	-58.33%
870 nm	0.054	0.0811	-0.027	-50.17%
		RMS 1:8	0.071	

	Wiggins 4/27/05 – 17:00			
	ASR 26	NSP	Difference	Percent Difference
Band	Generated	Generated	ASR-NSP	1 - (NSP/ASR)
380 nm	0.525	0.5411	-0.016	-3.08%
400 nm	0.417	0.5784	-0.161	-38.70%
440 nm	0.316	0.3149	0.001	0.35%
520 nm	0.208	0.2056	0.002	1.16%
610 nm	0.149	0.1744	-0.025	-17.02%
670 nm	0.097	0.1275	-0.031	-31.49%
780 nm	0.06	0.0906	-0.031	-51.00%
870 nm	0.054	0.0767	-0.023	-42.12%
		RMS 1:8	0.061	

	Wiggins 4/27/05 – 17:10			
	ASR 26	NSP	Difference	Percent Difference
Band	Generated	Generated	ASR-NSP	1 - (NSP/ASR)
380 nm	0.525	0.5585	-0.034	-6.39%
400 nm	0.417	0.5942	-0.177	-42.48%
440 nm	0.316	0.3264	-0.010	-3.29%
520 nm	0.208	0.2134	-0.005	-2.57%
610 nm	0.149	0.1803	-0.031	-21.00%
670 nm	0.097	0.1324	-0.035	-36.52%
780 nm	0.06	0.0935	-0.034	-55.88%
870 nm	0.054	0.0781	-0.024	-44.69%
		RMS 1:8	0.068	

	Wiggins 4/27/05 – 17:25			
	ASR 26	NSP	Difference	Percent Difference
Band	Generated	Generated	ASR-NSP	1 - (NSP/ASR)
380 nm	0.525	0.5668	-0.042	-7.97%
400 nm	0.417	0.6007	-0.184	-44.06%
440 nm	0.316	0.3284	-0.012	-3.93%
520 nm	0.208	0.2137	-0.006	-2.76%
610 nm	0.149	0.1802	-0.031	-20.93%
670 nm	0.097	0.1325	-0.035	-36.58%
780 nm	0.06	0.0928	-0.033	-54.65%
870 nm	0.054	0.0776	-0.024	-43.61%
		RMS 1:8	0.070	

A.5.2. Optical Depth, ASR 27

	Wiggins 4/27/05 – 16:30			
	ASR 27	NSP	Difference	Percent Difference
Band	Generated	Generated	ASR-NSP	1 - (NSP/ASR)
380 nm	0.504	0.5902	-0.086	-17.10%
400 nm	0.441	0.5549	-0.114	-25.82%
440 nm	0.323	0.3398	-0.017	-5.19%
520 nm	0.197	0.2127	-0.016	-7.97%
610 nm	0.155	0.1885	-0.034	-21.62%
670 nm	0.106	0.1313	-0.025	-23.87%
780 nm	0.066	0.0968	-0.031	-46.67%
870 nm	0.044	0.0799	-0.036	-81.52%
		RMS 1:8	0.056	

	Wiggins 4/27/05 – 16:40			
	ASR 27	NSP	Difference	Percent Difference
Band	Generated	Generated	ASR-NSP	1 - (NSP/ASR)
380 nm	0.504	0.5917	-0.088	-17.39%
400 nm	0.441	0.5574	-0.116	-26.39%
440 nm	0.323	0.3412	-0.018	-5.63%
520 nm	0.197	0.2135	-0.016	-8.36%
610 nm	0.155	0.1891	-0.034	-22.03%
670 nm	0.106	0.1317	-0.026	-24.27%
780 nm	0.066	0.0961	-0.030	-45.57%
870 nm	0.044	0.0783	-0.034	-78.05%
		RMS 1:8	0.057	

	Wiggins 4/27/05 – 16:50			
	ASR 27	NSP	Difference	Percent Difference
Band	Generated	Generated	ASR-NSP	1 - (NSP/ASR)
380 nm	0.504	0.5865	-0.083	-16.37%
400 nm	0.441	0.5544	-0.113	-25.70%
440 nm	0.323	0.3389	-0.016	-4.92%
520 nm	0.197	0.2121	-0.015	-7.64%
610 nm	0.155	0.1889	-0.034	-21.84%
670 nm	0.106	0.1314	-0.025	-24.00%
780 nm	0.066	0.0966	-0.031	-46.43%
870 nm	0.044	0.0787	-0.035	-78.84%
		RMS 1:8	0.055	

	Wiggins 4/27/05 – 17:00			
	ASR 27	NSP	Difference	Percent Difference
Band	Generated	Generated	ASR-NSP	1 - (NSP/ASR)
380 nm	0.504	0.5776	-0.074	-14.61%
400 nm	0.441	0.5311	-0.090	-20.42%
440 nm	0.323	0.3206	0.002	0.73%
520 nm	0.197	0.2007	-0.004	-1.90%
610 nm	0.155	0.1814	-0.026	-17.05%
670 nm	0.106	0.1255	-0.020	-18.40%
780 nm	0.066	0.0923	-0.026	-39.84%
870 nm	0.044	0.0743	-0.030	-68.94%
		RMS 1:8	0.045	

	Wiggins 4/27/05 – 17:10			
	ASR 27	NSP	Difference	Percent Difference
Band	Generated	Generated	ASR-NSP	1 - (NSP/ASR)
380 nm	0.504	0.5752	-0.071	-14.13%
400 nm	0.441	0.5465	-0.105	-23.92%
440 nm	0.323	0.3322	-0.009	-2.85%
520 nm	0.197	0.2085	-0.012	-5.85%
610 nm	0.155	0.1874	-0.032	-20.93%
670 nm	0.106	0.1303	-0.024	-22.95%
780 nm	0.066	0.0950	-0.029	-43.98%
870 nm	0.044	0.0757	-0.032	-72.13%
		RMS 1:8	0.050	

	Wiggins 4/27/05 – 17:25			
	ASR 27	NSP	Difference	Percent Difference
Band	Generated	Generated	ASR-NSP	1 - (NSP/ASR)
380 nm	0.504	0.5837	-0.080	-15.81%
400 nm	0.441	0.5524	-0.111	-25.25%
440 nm	0.323	0.3343	-0.011	-3.49%
520 nm	0.197	0.2090	-0.012	-6.11%
610 nm	0.155	0.1874	-0.032	-20.90%
670 nm	0.106	0.1304	-0.024	-23.02%
780 nm	0.066	0.0945	-0.029	-43.18%
870 nm	0.044	0.0751	-0.031	-70.72%
		RMS 1:8	0.053	

A.5.3. Optical Depth, MFRSR 477

	Wiggins 4/27/05 – 16:30			
	MFR 477	NSP	Difference	Percent Difference
Band	Generated	Generated	MFRSR-NSP	1 - (NSP/MFRSR)
415 nm	0.422	0.4718	-0.050	-11.79%
500 nm	0.236	0.2655	-0.029	-12.49%
615 nm	0.164	0.1795	-0.016	-9.47%
673 nm	0.109	0.1342	-0.025	-23.09%
870 nm	0.053	0.0766	-0.024	-44.52%
		RMS 1:5	0.031	

	Wiggins 4/27/05 – 16:40			
	MFR 477	NSP	Difference	Percent Difference
Band	Generated	Generated	MFRSR-NSP	1 - (NSP/MFRSR)
415 nm	0.422	0.4740	-0.052	-12.32%
500 nm	0.236	0.2671	-0.031	-13.17%
615 nm	0.164	0.1801	-0.016	-9.83%
673 nm	0.109	0.1347	-0.026	-23.59%
870 nm	0.053	0.0749	-0.022	-41.27%
		RMS 1:5	0.032	

	Wiggins 4/27/05 – 16:50			
	MFR 477	NSP	Difference	Percent Difference
Band	Generated	Generated	MFRSR-NSP	1 - (NSP/MFRSR)
415 nm	0.422	0.4714	-0.049	-11.71%
500 nm	0.236	0.2655	-0.029	-12.50%
615 nm	0.164	0.1797	-0.016	-9.60%
673 nm	0.109	0.1345	-0.026	-23.42%
870 nm	0.053	0.0749	-0.022	-41.29%
		RMS 1:5	0.031	

	Wiggins 4/27/05 – 17:00			
	MFR 477	NSP	Difference	Percent Difference
Band	Generated	Generated	MFRSR-NSP	1 - (NSP/MFRSR)
415 nm	0.422	0.4497	-0.028	-6.57%
500 nm	0.236	0.2529	-0.017	-7.16%
615 nm	0.164	0.1723	-0.008	-5.05%
673 nm	0.109	0.1288	-0.020	-18.20%
870 nm	0.053	0.0709	-0.018	-33.75%
		RMS 1:5	0.019	

	Wiggins 4/27/05 – 17:10			
	MFR 477	NSP	Difference	Percent Difference
Band	Generated	Generated	MFRSR-NSP	1 - (NSP/MFRSR)
415 nm	0.422	0.4638	-0.042	-9.91%
500 nm	0.236	0.2619	-0.026	-10.96%
615 nm	0.164	0.1782	-0.014	-8.64%
673 nm	0.109	0.1334	-0.024	-22.43%
870 nm	0.053	0.0726	-0.020	-36.94%
		RMS 1:5	0.027	

	Wiggins 4/27/05 – 17:25			
	MFR 477	NSP	Difference	Percent Difference
Band	Generated	Generated	MFRSR-NSP	1 - (NSP/MFRSR)
415 nm	0.422	0.4683	-0.046	-10.96%
500 nm	0.236	0.2629	-0.027	-11.41%
615 nm	0.164	0.1780	-0.014	-8.56%
673 nm	0.109	0.1339	-0.025	-22.83%
870 nm	0.053	0.0716	-0.019	-35.09%
		RMS 1:5	0.028	

A.5.4. Diffuse-to-Global Ratio, MFRSR 477

	Wiggins 4/27/05 – 16:30			
	MFR 477	NSP	Difference	Percent Difference
Band	Generated	Generated	MFRSR-NSP	1 - (NSP/MFRSR)
415 nm	0.2478	0.2268	0.021	8.48%
500 nm	0.1498	0.1357	0.014	9.41%
615 nm	0.086	0.0779	0.008	9.40%
673 nm	0.0688	0.0602	0.009	12.54%
870 nm	0.0563	0.0456	0.011	18.98%
		RMS 1:5	0.013	

	Wiggins 4/27/05 – 16:40			
	MFR 477	NSP	Difference	Percent Difference
Band	Generated	Generated	MFRSR-NSP	1 - (NSP/MFRSR)
415 nm	0.2461	0.2227	0.023	9.49%
500 nm	0.1491	0.1332	0.016	10.67%
615 nm	0.0859	0.0758	0.010	11.70%
673 nm	0.0688	0.0581	0.011	15.50%
870 nm	0.0564	0.0439	0.013	22.21%
		RMS 1:5	0.015	

	Wiggins 4/27/05 – 16:50			
	MFR 477	NSP	Difference	Percent Difference
Band	Generated	Generated	ASR-NSP	1 - (NSP/ASR)
415 nm	0.2437	0.2184	0.025	10.38%
500 nm	0.1489	0.1300	0.019	12.68%
615 nm	0.0854	0.0736	0.012	13.85%
673 nm	0.0685	0.0562	0.012	17.96%
870 nm	0.0564	0.0421	0.014	25.33%
		RMS 1:5	0.017	

	Wiggins 4/27/05 – 17:00			
	MFR 477	NSP	Difference	Percent Difference
Band	Generated	Generated	MFRSR-NSP	1 - (NSP/MFRSR)
415 nm	0.2411	0.1990	0.042	17.47%
500 nm	0.1464	0.1180	0.028	19.38%
615 nm	0.0847	0.0668	0.018	21.11%
673 nm	0.068	0.0512	0.017	24.70%
870 nm	0.0564	0.0392	0.017	30.59%
		RMS 1:5	0.026	

	Wiggins 4/27/05 – 17:10			
	MFR 477	NSP	Difference	Percent Difference
Band	Generated	Generated	MFRSR-NSP	1 - (NSP/MFRSR)
415 nm	0.2387	0.2061	0.033	13.67%
500 nm	0.145	0.1231	0.022	15.12%
615 nm	0.0839	0.0703	0.014	16.18%
673 nm	0.0674	0.0541	0.013	19.68%
870 nm	0.0563	0.0409	0.015	27.43%
		RMS 1:5	0.021	

	Wiggins 4/27/05 – 17:25			
	MFR 477	NSP	Difference	Percent Difference
Band	Generated	Generated	MFRSR-NSP	1 - (NSP/MFRSR)
415 nm	0.2369	0.2041	0.033	13.83%
500 nm	0.1439	0.1205	0.023	16.23%
615 nm	0.0834	0.0681	0.015	18.37%
673 nm	0.067	0.0521	0.015	22.18%
870 nm	0.0563	0.0397	0.017	29.43%
		RMS 1:5	0.022	

This page intentionally blank

Appendix B. LED Calibration System Circuit Design Schematic

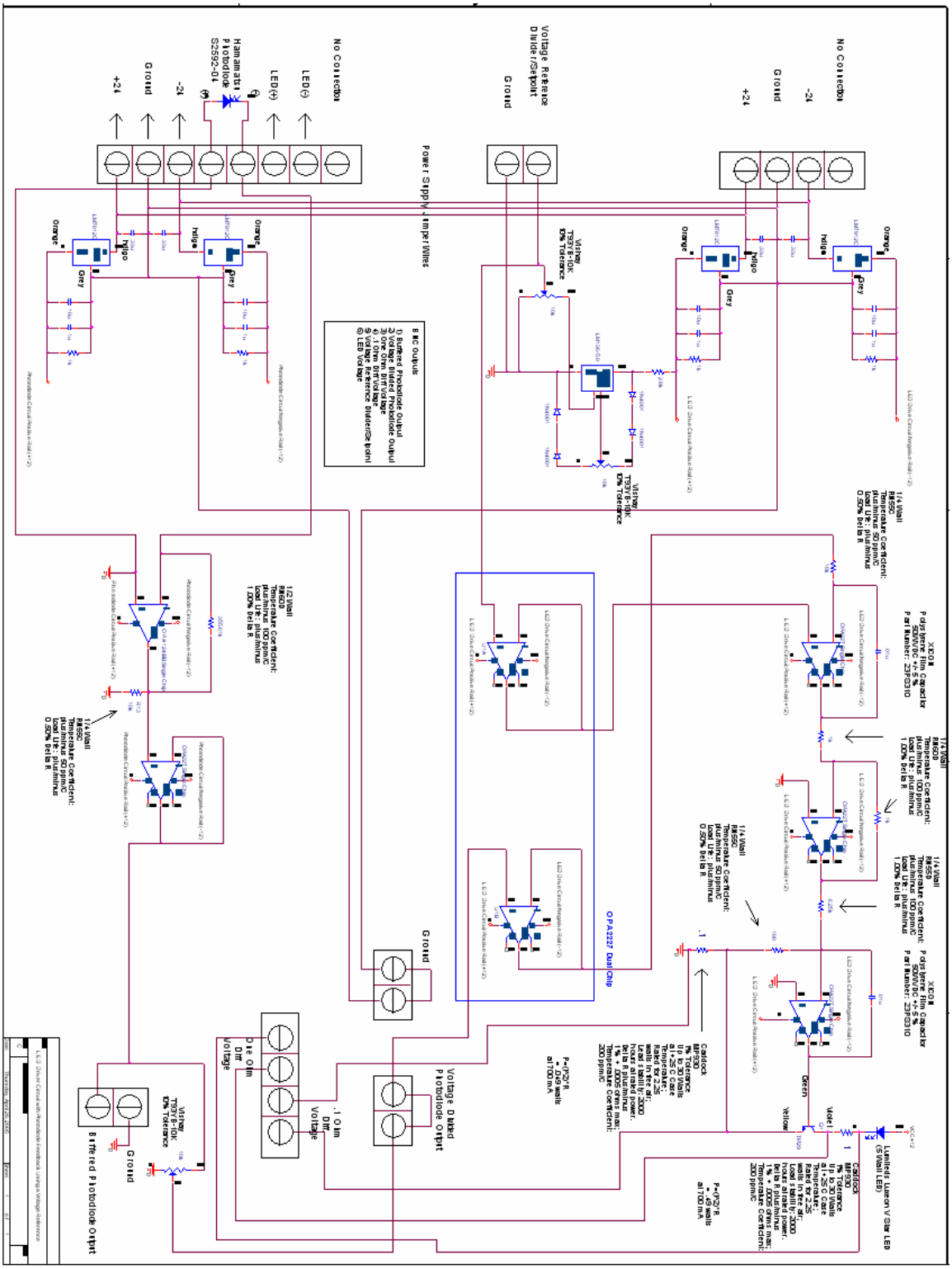

REPORT DOCUMENTATION PAGE

Form Approved
OMB No. 0704-0188

The public reporting burden for this collection of information is estimated to average 1 hour per response, including the time for reviewing instructions, searching existing data sources, gathering and maintaining the data needed, and completing and reviewing the collection of information. Send comments regarding this burden estimate or any other aspect of this collection of information, including suggestions for reducing this burden, to Department of Defense, Washington Headquarters Services, Directorate for Information Operations and Reports (0704-0188), 1215 Jefferson Davis Highway, Suite 1204, Arlington, VA 22202-4302. Respondents should be aware that notwithstanding any other provision of law, no person shall be subject to any penalty for failing to comply with a collection of information if it does not display a currently valid OMB control number.
PLEASE DO NOT RETURN YOUR FORM TO THE ABOVE ADDRESS.

1. REPORT DATE *(DD-MM-YYYY)*	2. REPORT TYPE	3. DATES COVERED *(From - To)*
10-02-2006	Verification and Validation Report	Sept 2003 - Jan 2006

4. TITLE AND SUBTITLE
Novel Hyperspectral Sun Photometer for Satellite Remote Sensing Data Radiometric Calibration and Atmospheric Aerosol Studies

5a. CONTRACT NUMBER
NASA Task Order NNS04AB54T

5b. GRANT NUMBER

5c. PROGRAM ELEMENT NUMBER

6. AUTHOR(S)
Mary Pagnutti (1)
Robert E. Ryan (1)
Kara Holekamp (1)
Gary Harrington (1)
Troy Frisbie (2)

5d. PROJECT NUMBER
SWR CB10-2005-00

5e. TASK NUMBER

5f. WORK UNIT NUMBER

7. PERFORMING ORGANIZATION NAME(S) AND ADDRESS(ES)
(1) Science Systems and Applications, Inc., Bldg. 1105, John C. Stennis Space Center, MS 39529
(2) Applied Sciences Directorate, National Aeronautics and Space Administration, Code MA00, Bldg. 1100, John C. Stennis Space Center, MS 39529

8. PERFORMING ORGANIZATION REPORT NUMBER

9. SPONSORING/MONITORING AGENCY NAME(S) AND ADDRESS(ES)
Applied Research & Technology Project Office, National Aeronautics and Space Administration, Code MA00, Bldg. 1100, John C. Stennis Space Center, MS 39529

10. SPONSORING/MONITOR'S ACRONYM(S)
NASA ASD

11. SPONSORING/MONITORING REPORT NUMBER
SSTI-2220-0063

12. DISTRIBUTION/AVAILABILITY STATEMENT
Unclassified/Publicly available STI per NASA Form 1676

13. SUPPLEMENTARY NOTES
NASA Verification and Validation Report for public release through Applications Implementation Working Group (AIWG) Web site at http://aiwg.gsfc.nasa.gov/

14. ABSTRACT

A simple and cost-effective, hyperspectral sun photometer for radiometric vicarious remote sensing system calibration, air quality monitoring, and potentially in-situ planetary climatological studies, was developed. The device was constructed solely from off the shelf components and was designed to be easily deployable for support of short-term verification and validation data collects. This sun photometer not only provides the same data products as existing multi-band sun photometers but also the potential of hyperspectral optical depth and diffuse-to-global products. As compared to traditional sun photometers, this device requires a simpler setup, less data acquisition time and allows for a more direct calibration approach. Fielding this instrument has also enabled Stennis Space Center (SSC) Applied Sciences Directorate personnel to cross-calibrate existing sun photometers. This innovative research will position SSC personnel to perform air quality assessments in support of the NASA Applied Sciences Program's National Applications program element as well as to develop techniques to evaluate aerosols in a Martian or other planetary atmosphere.

15. SUBJECT TERMS
solar irradiance, Martian studies, sun photometer, verification and validation

16. SECURITY CLASSIFICATION OF:			17. LIMITATION OF ABSTRACT	18. NUMBER OF PAGES	19b. NAME OF RESPONSIBLE PERSON
a. REPORT	b. ABSTRACT	c. THIS PAGE			Troy E. Frisbie
					19b. TELEPHONE NUMBER *(Include area code)*
U	U	U	UU	47	(228) 688-1989